Dissertations
Department of Chemistry
University of Eastern Finland

No. 143 (2017)

Dau Thuy Minh

Luminescent coinage metal complexes based on multidentate phosphine ligands

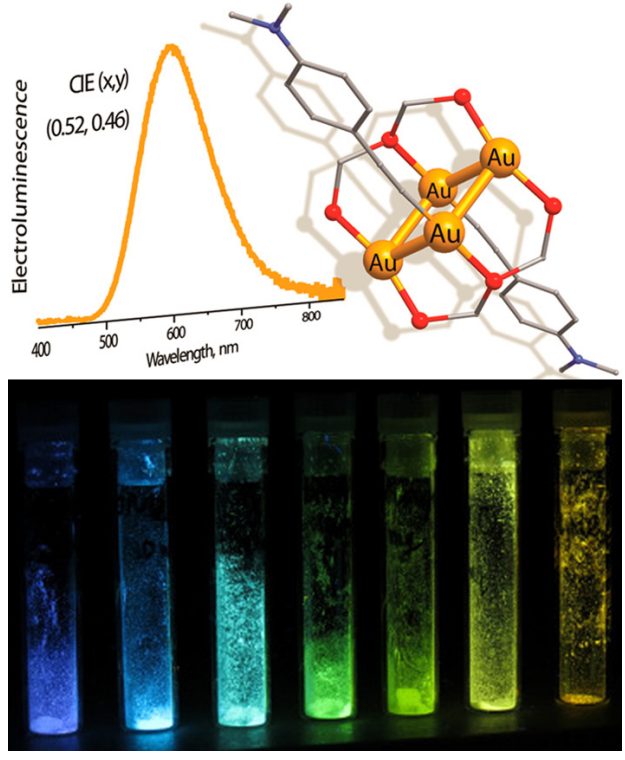

Luminescent coinage metal complexes based on multidentate phosphine ligands

Dau Thuy Minh

Department of Chemistry

University of Eastern Finland

Joensuu 2017

Dau Thuy Minh

Department of Chemistry, University of Eastern Finland

P.O. Box 111, FI-80101 Joensuu, Finland

Email: minh.dau@uef.fi

Supervisor

Prof. Igor O. Koshevoy, Department of Chemistry, University of Eastern Finland.

Referees

Prof. Pascual Lahuerta, University of Valencia.
Prof. Heikki Tuononen, University of Jyväskylä.

Opponent

PD (Privatdozent) Dr. Andreas Steffen, Institute of Inorganic Chemistry, Julius Maximilians University, Würzburg.

To be presented, with the permission of the Faculty of Science and Forestry of the University of Eastern Finland, for public criticism in Auditorium F101, Yliopistokatu 7, Joensuu, on 12th December, 2017, at 12 noon.

ISBN: 978-952-61-2663-0

ISSN: 2242-1033

Grano Oy

Joensuu 2017

ABSTRACT

In addition to their impressive monetary, jewelry and metallurgical values, from a historical perspective, coinage metals, which comprise the copper, silver, and gold triad, have attracted extensive research attention due to the chemical reactivity and physical properties of these metals' derivatives. Numerous studies, in this aspect, have been related to the closed-shell d^{10}–d^{10} interactions found among the complexes of coinage metals in an oxidation state +1. These non-covalent metal-metal contacts, which are supported by a variety of stereochemically suitable ligands, are a key factor that define the unprecedented structural diversity of d^{10}-containing species, in addition to their fascinating photophysical properties.

The effects of ancillary alkynyl ligands have been studied within a series of gold(I) complexes stabilized by the linear-type triphosphine (PPP). These tetranuclear clusters adopt two structural motifs (rhomboidal and unprecedented T-shaped arrangements of metal ions), which subtly depend on the intrinsic features of organic alkynyl constituents. Altering the electronic properties of the ligand sphere provides a facile way to tune the solid state optical behaviour of these compounds, which exhibit room temperature luminescence over a broad range of the visible spectrum. As proof of this concept, and for the first time among gold(I) clusters, the most intensely emissive complex was employed as a dopant phosphorescent emitter in an organic light-emitting diode, thus confirming the promising potential for utilization of polynuclear d^{10} compounds in electroluminescent devices.

Furthermore, the synthesis of homoleptic compounds, which are based on tri- and congener tetradentate congener phosphine ligands (PPP and PPPP), was carried out to produce a set of homo- and heteronuclear d^{10} metal species, consisting of Cu^{I}, Ag^{I} and Au^{I} ions. Depending on the ligand denticity, the metal cores revealed linear (PPP) or planar star-shaped (PPPP) cluster cores with variable compositions of the constituent d^{10} centers. The negligible contribution of the phosphines into excited states, as indicated by theoretical modeling, allowed one to predominantly correlate the observed moderate to strong phosphorescence with the nature of the metal frameworks.

To extend insight into the influence of phosphine coordinating properties on the assembly of the d^{10} cluster motifs, the heterodentate hemilabile ligand (P(PO)P) was utilized for the development of low nuclearity coinage metal compounds. Combination of hard (oxygen) and soft (phosphorus) donor functions controls the molecular structure as it offers a variable binding capacity, which efficiently adapts to the preferred coordination stereochemistry of the constituent metal atoms. The luminescence behaviour of these complexes depends on both the composition of metal frameworks and on the ligand bonding character, including the delicate influence of the weakly bound P-oxide function.

In conclusion, a diverse family of small coinage metal clusters was designed *via* the use of a selection of multidentate phosphines, which efficiently govern the composition and geometry of the metal core. The evaluated relationships between the molecular stereochemistry and the photophysical properties form an important basis for the development of novel, metal-rich photofunctional materials.

LIST OF ORIGINAL PUBLICATIONS

This thesis is based on data presented in the following articles, referred to by the Roman numerals I-V.

I Dau, T. M. ; Chen, Y.-A.; Karttunen, A. J.; Grachova, E. V.; Tunik, S. P.; Lin, K.-T.; Hung, W.-Y.; Chou, P. T.; Pakkanen, T. A.; Koshevoy, I. O., Tetragold(I) Complexes: Solution Isomerization and Tunable Solid-State Luminescence, Inorg. Chem., **2014**, 53 (24), 12720–12731

II Dau, T. M. ; Shakirova, J. R.; Doménech, A.; Jänis, J.; Haukka, M.; Grachova, E. V.; Pakkanen, T. A.; Tunik, S. P.; Koshevoy, I. O., Ferrocenyl-Functionalized Tetranuclear Gold(I) and Gold(I)–Copper(I) Complexes Based on Tridentate Phosphanes, Eur. J. Inorg. Chem. **2013**, 4976–4983.

III Dau, M. T.; Shakirova, J. R.; Karttunen, A. J.; Grachova, E. V.; Tunik, S. P.; Melnikov, A. S.; Pakkanen, T. A.; Koshevoy, I. O., Coinage Metal Complexes Supported by the Tri- and Tetraphosphine Ligands, Inorg. Chem. **2014**, 53, 4705−4715.

IV Dau, T. M. ; Asamoah, B. D.; Belyaev, A.; Chakkaradhari, G.; Hirva, P.; Jänis, J.; Grachova, E. V.; Tunik, S. P.; Koshevoy, I. O., Adjustable coordination of a hybrid phosphine–phosphine oxide ligand in luminescent Cu, Ag and Au complexes, Dalton Trans. **2016**, 45, 14160–14173.

V Belyaev, A.; Dau, T. M.; Jänis, J.; Grachova, E. V.; Tunik, S. P.; Koshevoy, I. O., Low-Nuclearity Alkynyl d^{10} Clusters Supported by Chelating Multidentate Phosphines, Organometallics **2016**, 35, 3763−3774.

AUTHOR'S CONTRIBUTION

The author conducted the preparation of the novel compounds described in the thesis and their crystallographic analysis (all the complexes in publications I, III; complexes **3** and **4** in publication II, complexes **1**−**10** in publication IV; complexes **13**−**15** in publication V), the NMR spectroscopic measurements for publications IV, V, and interpreted the corresponding results of advanced NMR experiments performed elsewhere. The author participated in analyzing the photophysical and computational results and in writing the publications I–V.

CONTENTS

LIST OF ABBREVIATIONS

CV	Cyclic voltammetry
DFT	Density functional theory
DMSO	Dimethyl sulfoxide
EL	Electroluminescence
EQE	External quantum efficiency
ESI-MS	Electrospray ionization mass spectrometry
HOMO	Highest occupied molecular orbital
HSOMO	Highest singly occupied molecular orbital
IL	Intra ligand
LLCT	Ligand-ligand charge transfer
LMCT	Ligand-metal charge transfer
LUMO	Lowest unoccupied molecular orbital
MLCT	Metal-ligand charge transfer
MXLCT	Metal-halide-ligand charge transfer
NMR	Nuclear magnetic resonance
OLED	Organic-light-emitting-diode
P(PO)P	Bis(2-(diphenylphosphino)phenyl phosphine oxide
PPP	Bis(diphenylphosphinomethyl)-phenylphosphine, dpmp
PPPP	Tris(diphenyl-phosphinomethyl)phosphine
SOMO	Single occupied molecular orbital
SWV	Square wave voltammetry
XRD	X-ray diffraction

1 INTRODUCTION

Do you know that the medals of the Nobel Prize have been made of gold-plated green gold for several decades?[1] What is green gold? Green gold, also known as electrum, is composed of gold, silver and small amounts of copper and other metals.

Dating back to the beginning of the 6th century BC, electrum was used to form the first-ever metal coins. Hence, the metals in group 11 of the periodic table, which comprise copper, silver and gold, have been utilized throughout ancient and modern civilizations. They are called coinage- or noble metals. What makes them so precious?

Historically, copper (cuprum) has been used in human life for the longest time among these three metals, due to its abundance in nature, versatility and low cost. The first uses of copper date back to 5000 BC. It has been utilized in a wide range of applications, e.g. as currency, in construction (copper alloys, copper wires), in automotive production, in electronics and in telecommunications.

Unlike copper, silver (argentum) is a real precious metal, which is why we find silver used in many expessions for solemn events in our lives, such as *"silver anniversary"* or *"born with a silver spoon"* , in order to emphasize their value. Silver is famous for its use in jewelry and silverware, photography and brazing alloys.

The top precious metal, which was discovered as shiny yellow nuggets, is gold (aurum). Gold has traditionally been an attribute of power, beauty, and the cultural elite due to its high value and chemical resistance. It has been widely used in currency, jewelry, electronics (electrical contacts and connectors in highly humid/corrosive atmospheres and wires in high-energy fields) and medicine (anti-inflammatory, anti-tumor agents and restorative dentistry).

From a chemical viewpoint, the valence electron configurations of atoms and ions are essential. For copper, silver and gold atoms, these are termed as $3d^{10}4s^1$, $4d^{10}5s^1$ and $5d^{10}6s^1$, respectively. Consequently, these metals in the oxidation state +1 form the closed shell d^{10} ions, which one might expect to be chemically inert. On the contrary, compounds containing Cu^I, Ag^I and Au^I ions demonstrate fascinating reactivity and particularly rich structural chemistry due to effective metal-metal interactions.

In fact, non-covalent d^{10}–d^{10} bonding, frequently encountered among coinage metal complexes, has played an important role in the design and construction of many supramolecular architectures, which exhibit appealing optical properties.[2] Starting from simple halide compounds, the chemistry of copper subgroup metals has developed into a large and diverse area with numerous applications in catalysis[3], biomedicine[4] and functional materials.[5,6,7]

1.1 METALLOPHILIC INTERACTIONS M(I)−M(I) IN GROUP 11 METAL COMPLEXES

Since the 1970s, the significance of the attraction between linearly two-coordinate gold(I) ions in gold(I) species has attracted considerable research attention.[8] The intra- or intermolecular Au–Au bonds were found for metal-metal separations in the range of *ca.* 2.7−3.3 Å, which are below the sum of van der Waals radii (3.4 Å).[2c,9] Because gold(I) centres have a closed-shell configuration ($5d^{10}$), which should allow weak van der Waals attraction only, the gold(I)–gold(I) interactions were considered to be a truly unexpected phenomenon.

In 1988, Schmidbaur introduced the term "aurophilic interaction", which was defined as *"the unprecedented affinity between gold atoms even with "closed-shell" electronic configurations and equivalent electrical charge"*.[10] The energy of aurophilic bonding for two gold atoms was estimated to range from 29 to 46 kJ/mol, which is comparable in strength to a hydrogen bond.[11]

In 1991, Pyykkö and Zhao[12] explained that gold(I)–gold(I) bonds were generated by correlation effects and strengthened by relativisitic effects. Later, Pyykkö[13] presented a deep theoretical analysis, according to which the nature of an aurophilic interaction d^{10}–d^{10} should be understood mainly as a dispersion effect.

The London dispersion forces are the attractive interactions of the short-lived dipoles, which are formed by unequal distribution of electrons, and interact with electron clouds of neighboring molecules to form more dipoles. The dispersion forces are proportional to the distance between the nucleus and electrons.[14] For the large atom of gold, the valence electrons are located far away from the nucleus, which makes them easy to polarize and, thus, to be involved in effective dispersion interactions. Therefore, gold(I) ions can interact with each other even though they have a closed electronic shell and equivalent positive charge.

On the other hand, among its neighbors in the periodic table, gold reveals a most pronounced tendency for relativistic effects, which simultaneously cause the contraction of the 6s and 6p orbitals, and the expansion of 5d orbitals. The reason for this effect, according to Gimeno and Laguna,[15] is to be found in the large positive charge of heavy Au nucleus; the electrons of gold atoms move in a high charge field, which leads to the velocities of the electrons approaching the speed of light. In addition, Pyykkö[16] has noted that the 6s orbital is exposed to a higher relativistic effect than the other shells, which causes an increase of relativistic mass and simultaneously the decrease of the orbital radius. Similarly, this approach can be applied to 6p orbitals.

The relativistic radial contraction and energetic stabilization make the valence d and f electrons more effectively shielded from the nucleus, thus the d and f orbitals are expanded.[17] Therefore, the energy difference between the empty 6s/6p orbitals and the filled-5d are reduced, indicating a more effective overlap and stronger gold(I)–gold(I) interactions (Fig. 1a).[9]

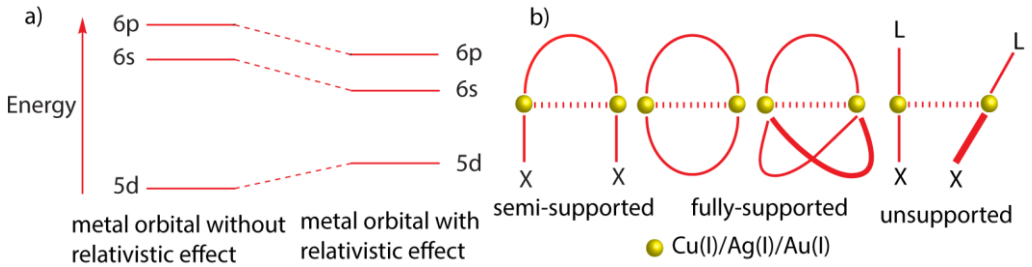

Figure 1. a) Energy-level diagram of atomic orbitals under the effect of the relativistic effect. b) Intramolecular and intermolecular metal-metal interactions.

A broader concept of *"metallophilic interaction"* was coined by Pyykkö and co-workers[18] as an analogy with aurophilicity. The metallophilic attractions, typically observed among closed-shell d^{10} ions of copper subgroup (Cu(I), Ag(I) and Au(I)) have been explained as a correlation-dispersion phenomenon, which is strengthened by the relativistic effect in the case of gold.[19] Futhermore, Laguna[20] deduced on the basis of theoretical calculations that *"the presence of only one gold atom is enough to induce metallophilic attractions in the group congeners and this effect could be modulated depending on the gold ligand"*. This conclusion is supported by the rich structural chemistry of Au–Cu and Au–Ag species.[21]

The bonding metal-metal distances are assumed to be smaller than the sums of the corresponding van der Waals radii. In general, Schmidbaur[22] classifies the metallophilic bonds into 2 types: intramolecular semi- and fully-supported bonds, and intermolecular unsupported contacts (Fig. 1b). Both types of metallophilic interactions play a key role in the construction of various structural patterns and therefore govern the design of discrete molecular clusters and supramolecular aggregates, which feature exceptional structural versatility.[2]

1.2 STRUCTURAL DIVERSITY AND MOLECULAR ENGINEERING: FROM SMALL COMPLEXES TO NANOSYSTEMS

The mononuclear d^{10} compounds can associate through the metal-metal contacts to form a variety of assemblies, such as dimers, oligomers and polymeric systems.

Generation of the polynuclear frameworks through metallophilic bonds is defined by coordination rules. Particularly, gold(I) ions preferrably adopt two coordinate geometry, while tri- and tetracoordination environments are predominant for copper(I) and silver(I) ions, not taking into account the metal-metal interactions. This

coordination discrepancy was explained by the larger deformation energy of a gold ligand sphere in comparison to those of monovalent copper and silver complexes.[23]

Beside the metal-metal bonds, the ligands, anions, and other external factors, such as solvents, temperature, and mechanical force can also affect the stereochemical peculiarities. The scope of this chapter focuses on the structural features mainly associated with metal-metal interactions, facilitated by a set of suitable ligands. The development of the multimetallic compounds follows the gradual progress that starts from small nuclearities such as di-, tri- and tetrametallic complexes and progress to high nuclearity clusters, infinite polymeric chains, supramolecular arrays, and finally, nanomaterials.

Dinuclear complexes

In comparison to semi- or fully supported intramolecular interactions, the unsupported intermolecular contacts in dinuclear complexes are very rare. Fernandez et al.[24] reported a bimetallic Au–Cu complex, in which the $[Au(C_6F_5)_2]^-$ anionic and the $[Cu(N{\equiv}C{-}CH_3)_2]^+$ cationic fragments are held together through a non-bridged Au–Cu bond (Fig. 2a).

The most common strategy for obtaining dinuclear complexes containing metal-metal interactions is to use bridging bidentate ligands. For instance, widely utilized diphosphine bis(diphenylphosphino)methane, dppm, (Fig. 2b) affords a dicoordinated gold complex $[\{Au(2\text{-}SC_6H_4NH_2)\}_2(\mu\text{-dppm})]$.[25]

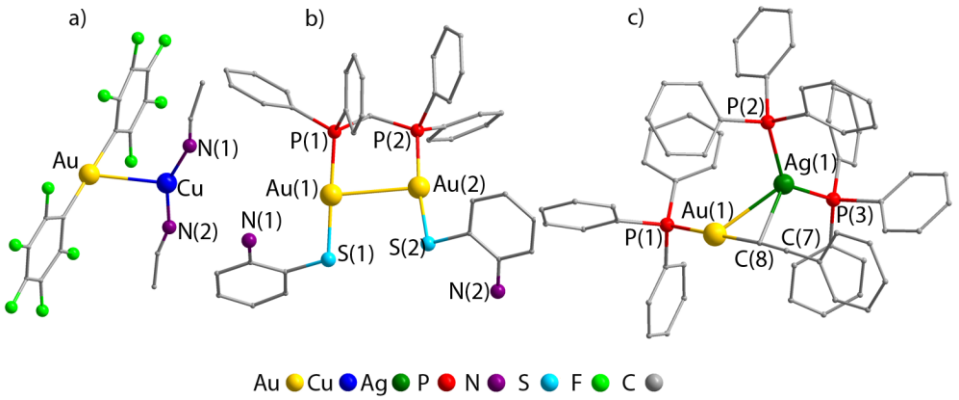

Figure 2. a) Unsupported Au–Cu interaction of dinuclear complex $[AuCu(C_6F_5)2(N{\equiv}C{-}CH_3)_2$.[24] b) Semi-supported Au–Au interaction of $[\{Au(2\text{-}SC_6H_4NH_2)\}_2(\mu\text{-dppm})]$.[25] c) The gold acetylide derivatives $[Au(C{\equiv}CPh)(PPh_3)]$.[26]

The metal-alkynyl compounds have been efficiently employed to trap other d^{10} metal ions through π-alkynyl coordination that illustrates a successful strategy for the preparation of a wide selection of di- and polynuclear coinage metal complexes. Figure 2c shows the dinuclear gold-silver complex, which was synthesized by utilizing the

high affinity of a coordinatively unsaturated silver(I) center to the gold acetylide derivative [Au(C≡CPh)(PPh_3)].[26]

Tri- and tetranuclear complexes

The tri-/tetranuclear complexes are usually obtained by using tri- or tetradentate ligands, which stabilize the corresponding nuclearity of the metal framework. For instance, tri- and tetraphosphine ligands support linear metal arrays in Ag(I) (Figure 3a) and Au(I) homoleptic complexes.[27,28] In some other cases, the heteropolydentate ligands can be used in combination with different binding groups, such as pyridine or carbene, which saturate the coordination requirements of the constituting metal ions. The tridentate ligand with two phosphorus and N-heterocyclic carbene (NHC) functions leads to the trinuclear gold(I) complex (Fig. 3b).[29] In the tetranuclear cluster $[Ag_4(P_2\text{-bpy})_2]I_2(BF_4)_2$ (P_2-bpy = 6,6-bis-(diphenylphosphinyl)-2,2'-bipyridine) (Fig. 3c), the hybrid tetradentate ligand involves a chelating bipyridine motif, functionalized with pendant phosphine groups, which support a flat tetrametallic core.[30]

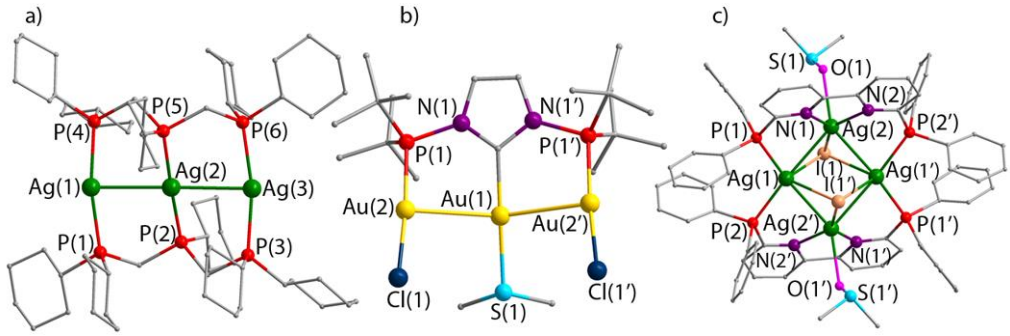

Figure 3. a) Trinuclear cation $[Ag_3(dcmp)]^{3+}$ (dcmp=bis(dicyclohexylphosphinomethyl)cyclohexylphosphine.[27] b) Trinuclear cation $[Au_3Cl_2(SMe_2)(PC_{NHC}P)]^+$.[29] c) Tetranuclear cation $[Ag_4(P_2\text{-bpy})_2I_2]^{2+}$ (P_2-bpy = 6,6-bis-(diphenylphosphinyl)-2,2'-bipyridine).[30]

The already mentioned approach, utilizing metallophilic bonding supported by π-alkynyl coordination for binding heterometal ions, serves as a promising method for the production of higher nuclearity aggregates, including the tri- and tetrametallic compounds. Some examples comprise the cationic clusters $[Au_3Cu(C_2R)_3(dpmp)]^+$ (R = 1-cyclohexanolyl) (Fig. 4a)[31] and $[Ag_2Au_2(\mu\text{-dpppy})_3(C{\equiv}CC_6H_5)_2]^{2+}$ (dpppy = 2,6-bis(diphenylphosphino)pyridine, Fig. 4b),[32] the arrangement of which is essentially determined by the stereochemical properties of the multidentate building blocks.

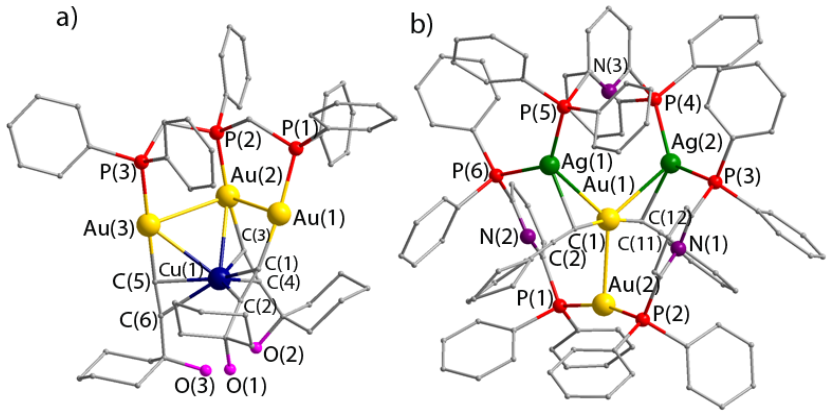

Figure 4. a) Tetranuclear $[Au_3Cu(C_2R)_3(dpmp)]^+$ (R = 1-cyclohexanolyl) cation.[31] b) Tetranuclear $[Ag_2Au_2(\mu\text{-dpppy})_3(C{\equiv}CC_6H_5)_2]^{2+}$.[32]

Higher nuclearity complexes, infinite chains and supramolecular arrays

The employment of polydentate ligands and/or the small ancillary binding groups, which support metallophilic interactions (like alkynyl or thiolate functions) open up wide oppoturnities for the design of various unconventional metal clusters of higher nuclearities. For instance, the series of octanuclear Au–M [M = Cu (Fig.5), Ag] complexes[31,33] have been assembled by means of templating triphosphine and auxiliary alkynyl ligands, which stabilize the resultant metal frameworks.

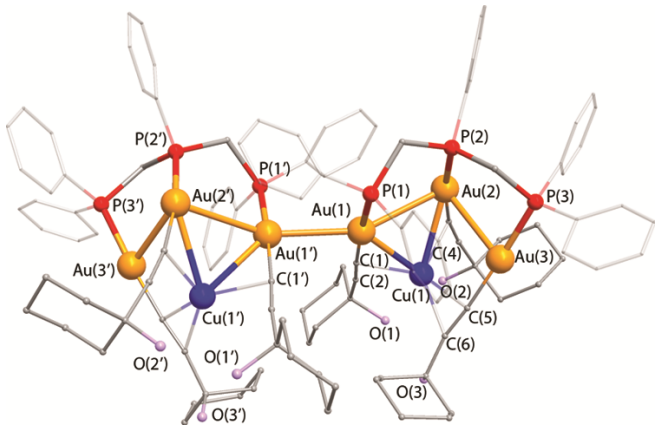

Figure 5. Octanuclear cation $[Au_6Cu_2(C_2C_6H_{11}O)_6(Ph_2PCH_2PPhCH_2PPh_2)_2]^{2+}$.[31]

The metallophilic interactions, which are not restricted by the ligand sphere, are capable of giving rise to the self-assembled structures, which contain ordered metal chains and extended 2D/3D supramolecular arrays. A coordination polymer of $[Cu(pyrazine)][Au(CN)_2]_2$ illustrates a 3D network, which is supported by aurophilic bonds (Fig. 6a).[34]

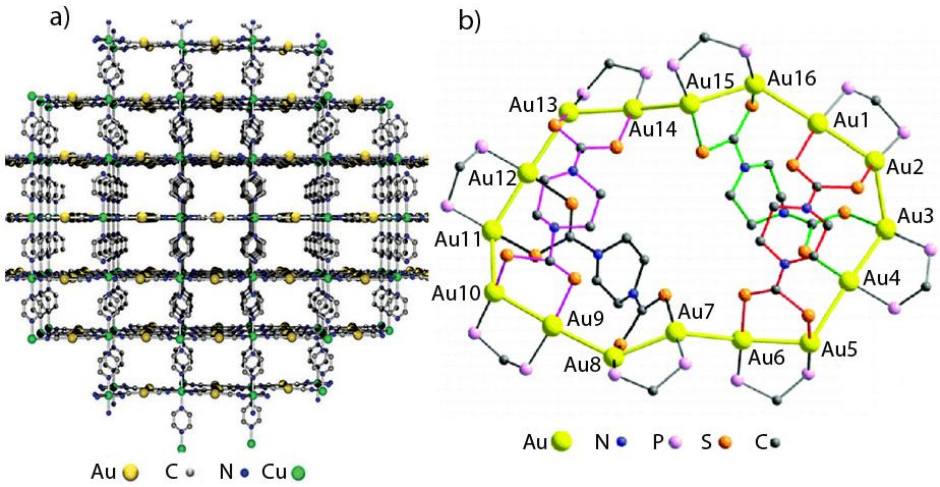

Figure 6. a) A network of $[Cu(pyrazine)][Au(CN)_2]_2$.[34] b) The Au_{16} rings connected through Au−Au interactions of a $[(dppm)_2Au_4(pipzdtc)]_4(PF_6)_8$ cluster.[35]

In addition, the polynuclear supramolecular structures, such as copper, silver and gold metallorings can be generated by the self-assembly of metal cluster units through metal-metal bonds. Among them, the gold rings are relatively rarer due to the more restricted coordination chemistry of monovalent gold(I) atoms. Fig. 6b displays the assembly of a chiral hexadecanuclear gold(I) cluster $[(dppm)_2Au_4(pipzdtc)]_4(PF_6)_8$ (dppm = bis-(diphenylphosphino)methane; pipzdtc = piperazine-1,4-dicarbodithiolate). The Au_{16} rings in this cluster are built up from four tetrametal units linked by aurophilic interactions.[35]

Nanomaterials

Furthermore, by using chemical reduction processes, the metal complexes can be transformed into atomically precise nanoparticles, which lead to well-defined nanomaterials. Thus, Wang, Q-M. et al.[36] and Zheng, N. et al.[37] synthesized interesting examples of heterometallic Au–Ag nanoclusters (Fig. 7) using sodium borohydride ($NaBH_4$) or a tert-butylamine borane complex as reducing agents.

The resultant large systems are stabilized by the three different types of bridging ligands or their combinations (phenylethynyl, 2-pyridylthiolate, and chloride), sometimes additionally supplemented by ancillary phosphines. Four kinds of surface motifs have been identified in $Au_{24}Ag_{20}$, $Au_{34}Ag_{28}$ and $Au_{80}Ag_{30}$ alkynyl clusters, where the linear PhC≡C–Au–C≡CPh staple connects from two to four metal atoms (Fig. 7d) *via* π-coordination of C≡C and extensive metallophilic interactions.

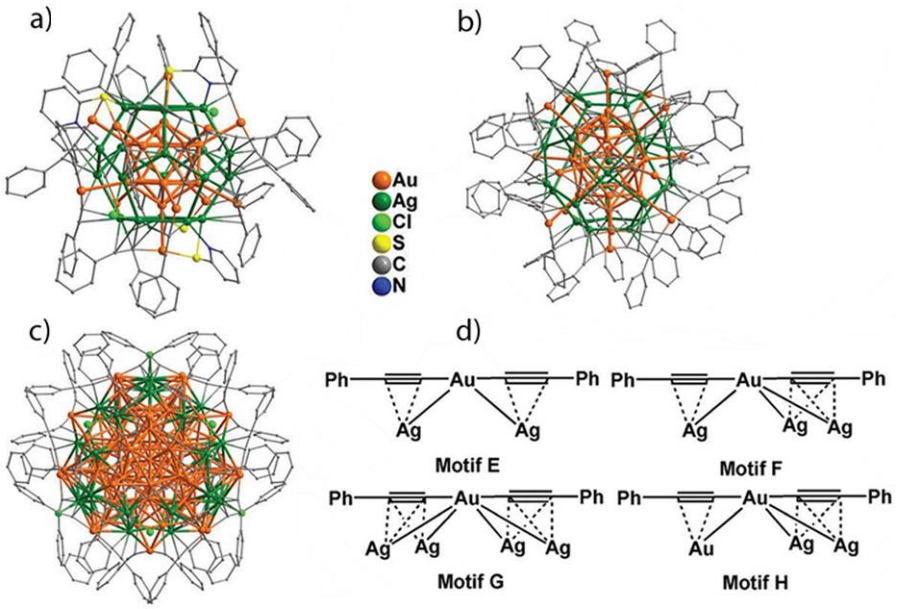

Figure 7. (a) Molecular structure of $Au_{24}Ag_{20}$; (b) molecular structure of $Au_{34}Ag_{28}$; (c) cationic part of $Au_{80}Ag_{30}$; (d) schematic representation of multiple coordination modes of linear PhC≡C–Au–C≡CPh staple.[36,37]

1.3. OPTICAL PROPERTIES: THE INFLUENCE OF LIGANDS AND METALLOPHILIC INTERACTIONS

The intriguing optical behaviour of the polynuclear coinage metal complexes is often assigned to the presence of extensive metallophilic bonding and variable structural arrangements of the metal frameworks.[38]

An example of modulation of the photophysical performance is given by two heterometallic gold-copper clusters $[Au_2Cu(C_6Cl_2F_3)_2(PPh_2py)_2][BF_4]$ and $[Au_2Cu(C_6Cl_2F_3)_2\{(PPh_2)_2phen\}(CH_3CN)][BF_4]$. In the solid state these cationic species exhibit a pronounced bathochromic shift of emission energy (up to 80 nm) with respect to their gold precursors $[Au(C_6Cl_2F_3)_2(PPh_2py)]$ and $[Au_2(C_6Cl_2F_3)_2\{(PPh_2)_2phen\}]$ upon binding the copper atom (Fig. 8a).[39] While the emissions of the homometallic Au complexes were assigned to the metal-perturbed intraligand transitions, those of the heteronuclear Au–Cu compounds were proposed to originate from a mixture of IL and MLCT transitions. This series highlights an important influence of the nature of the metal ions, which form the cluster cores, on the optical properties of this sort of d^{10} metal-rich molecular materials.

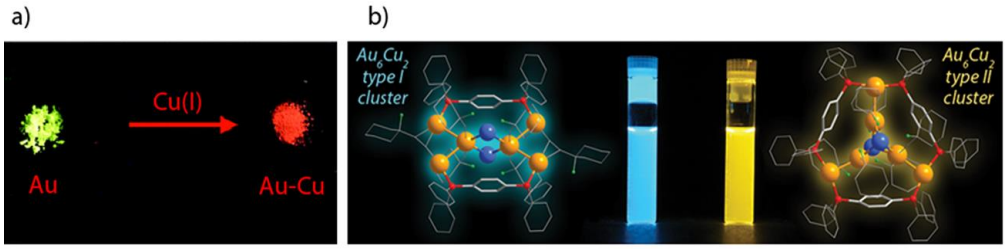

Figure 8. a) Copper-induced bathochromically shifted phosphorescence in Au(I)-Cu(I) heteronuclear complexes.[39] b) Distinctive emission of heteronuclear Au-Cu complexes directed by different geometries of metal cores.[40]

The photophysical performance is not only dependent on the composition but also on the geometry of the metal frameworks. Koshevoy et al.[40] reported two different types of structures for the octanuclear gold-copper complexes, which exhibited two distinct emissions. These structural motifs are mostly determined by the steric bulkiness and stereochemistry of the alkynyl ligands (Fig. 8b). The structure of type I, $[Au_6Cu_2(C_2R)_6(PP)_2]^{2+}$ (PP = 1,4-bis(diphenylphosphino)benzene), displayed light blue luminescence, which was assigned to Au→Au transitions mixed with certain contribution of charge transfer with Cu→Cu and d→π-alkynyl (MLCT) character. On the other hand, the structure of type II, $[Au_6Cu_2(C_2R)_6(PP)_3]^{2+}$, revealed a yellow emission, which originated from pure metal-centered transitions mostly localized within Cu ions.

As mentioned above, beside metallophilicity, ligands can have a pronounced influence on luminescent properties. In this case, the transitions involving both metal and ligand (MLCT or LMCT) charge transfers or transitions between the ligand π→π* orbitals (IL) can contribute to the emission of d^{10} complexes. Since ligands are usually responsible for bridging the metals to enhance the metal-metal bonds and stabilize the whole system, they siginificantly affect the geometries of compounds, and therefore govern the optical behaviour.

Chen et al.[41] introduced a series of Au_8Ag_4 alkynyl cluster complexes, which exhibited bright phosphorescence with a wide range of emission color, by modifying the electronic effects in aromatic acetylide ligands (Fig. 9). A blue shifted emission was observed for the electron-withdrawing CF_3 substituent in phenyl-acetylides and conversely, a red shift was detected in the case of electron-donating groups, such as Bu^t, OMe, or NMe_2. The phosphorescence was assigned to ^{3}LLCT/^{3}IL and Au_8Ag_4 cluster-centered ^{3}[d→p] transitions.

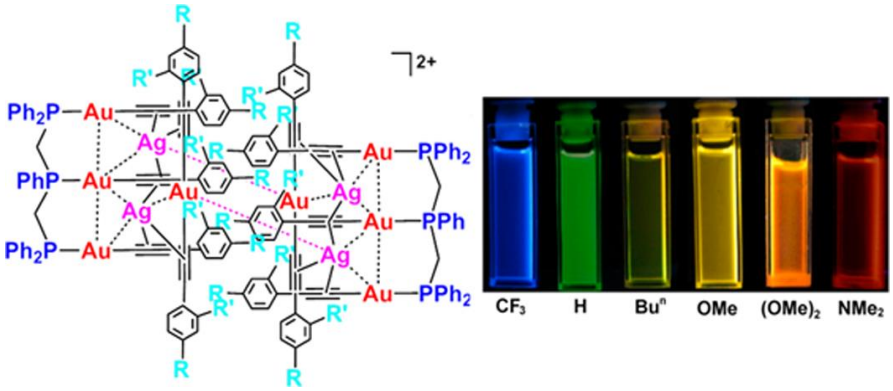

Figure 9. Luminescence of Au_8Ag_4 alkynyl cluster complexes in CH_2Cl_2 at room temperature.[41]

1.4 APPLICATIONS: ELECTROLUMINESCENCE (EL), IMAGING AND RESPONSIVE MATERIALS

Electroluminescence is regarded as an optical and electrical phenomenon, when a material generates light in response to an electrical current or a strong electrical field. Coinage-metal complexes, due to their intense and tunable emission, represent a promising class of luminophores, which are utilized in numerous applications, including organic-light emitting diodes (OLED),[42] chemosensing,[43] tumor treatment[4], bio-imaging[44] and stimuli-responsive photo-functional materials.[5,6,7]

Notably, a series of Au_4Ag_2 alkynyl clusters with high quantum yields of photoluminescence up to 62.5% were used as dopant emitters to fabricate OLEDs with high-performance.[42c] These devices achieved good EL with maximum current, power, and external quantum efficiencies of 24.1 cdA^{-1}, 11.6 lmW^{-1} and 7.0%, respectively.

Among other applications, luminescent bio-imaging is an actively growing area of research. This field covers a selection of methods, which require suitable photoactive molecular materials to visualize the biological objects, follow the dynamic processes or to measure a variety of analytes *in vitro* and *in vivo*, by monitoring the emission characteristics of the dyes. For static imaging, the phosphorescent clusters offer important advantages, not accessible with the conventional organic fluorophores, namely long emission lifetimes and high intensity, which is not quenched by molecular oxygen *via* a triplet-triplet annihilation mechanism. These properties allow for an easy and reliable detection of the target signal *via* the use of the time-gated technique that eliminates unwanted background fluorescence.[45] As proof of concept, a heterometallic complex $[Au_{14}Ag_4(C_2Ph)_{12}(PPh_2C_6H_4PPh_2)_6][PF_6]_4$, displays excellent phosphorescence behaviour and photostability, suited for both one- and two-photon-excited optical imaging in human stem cells. Embedding this cluster into silica gel nanoparticles for biocompatibility allowed their internalization into HeLa cells and the performance of time-resolved

fluorescent imaging (Fig. 10).[44b,44c]

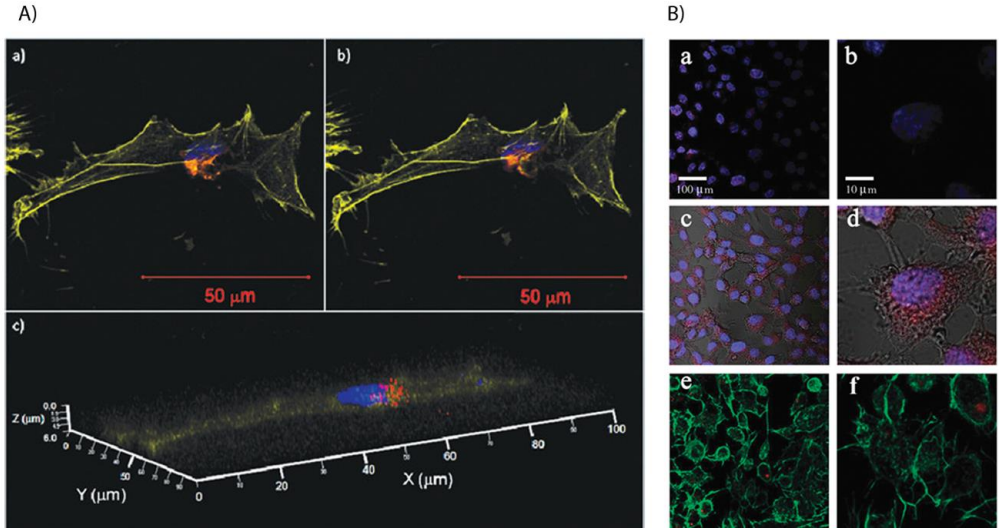

Figure 10. A) Confocal images of human mesenchymal stem cells incubated with silica encapsulated heterometallic Au-Ag cluster (red) overnight.[44b] B) Confocal fluorescence and overlaid fluorescence images of HeLa cells stained by the Au-Ag complex adduct (red) with DAPI (blue; images a–d) or FITC (green; images e, f).[44c]

Another practical employment of coinage-metal complexes stems from the mechano-, solvo-, vapo- or thermochromic alteration of optical characteristics. The phenomena summarized by the term "stimuli-responsive luminescence" can be described as the change of emission properties upon absorption of volatile organic compounds, applied *via* mechanical force or temperature variation. The distinct luminescence changes are conventionally associated with the modulation of metal-metal interactions,[5] metal-solvent contacts,[6] stacking, existence of different crystalline forms,[7] or crystal phase transitions.[5f,46] Stimuli-responsive photo-functional materials have rich potential for applications in memory devices, chemical sensors, and security inks. Fig. 11 displays a mechanochromic alteration of the emission of gold(I) isocyanide compounds *via* crystal-to-crystal transformation.[46]

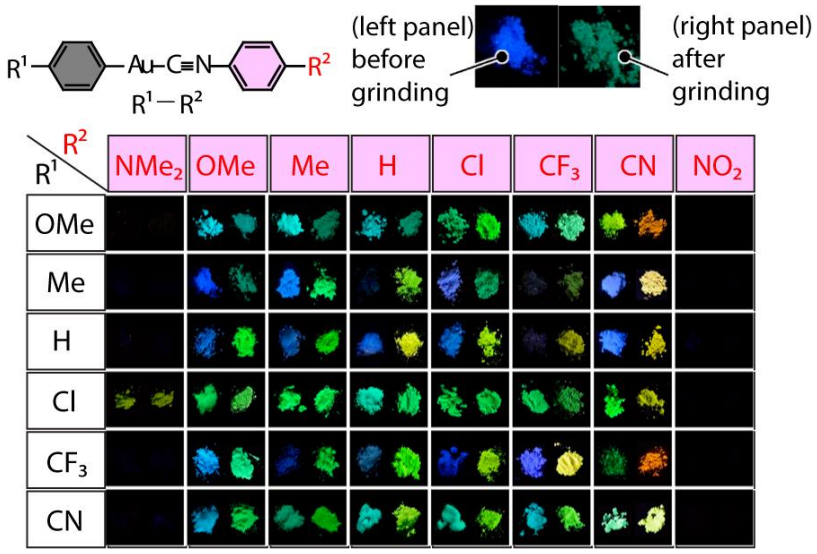

Figure 11. Mechanochromic luminescence of gold(I) isocyanide complexes featuring crystal-to-crystal phase transitions.[46]

1.5 AIMS OF THE STUDY

As has been outlined above, the combination of d^{10} metal-metal bonding together with the stabilizing effect of the ancillary ligands (alkynes, thiols, aryls) have been extensively utilized in construction of the homo- and heterometallic complexes. Both these grand factors have a significant influence on the physical behavior of gold-based compounds.[9,21b,38,43,47]

The first aim of this work was to perform the systematic alteration of the constituent alkynyl ligands in a small, gold-only cluster in an attempt to reveal the ligand effect on the structural features and simultaneously tailor their photo-physical properties. For this purpose, the triphosphine-supported tetragold motif was chosen due to the robust framework, facile formation and convenient functionalization *via* alkynyl building blocks.

The second direction was focused on the preparation of structurally congener small clusters, in order to vary the composition of the metal core and subsequently investigate the effect of the nature of the polynuclear metal center on the physical performance of the resultant species. To attain this goal, the stereo-chemically related tri- and tetraphosphine ligands were utilized for the synthesis of a rare series of d^{10} homoleptic compounds with a range of homo- and heterometal frameworks.

Ultimately, the third objective was to probe the effect of combining the heterodentate hard and soft donor functions on the coordinating ability of such a hybrid ligand, to investigate their influence on the assembly processes, on the structural and optical features of the low nuclearity cluster compounds, composed of the d^{10} ions with different coordination preferences.

2 EXPERIMENTAL

2.1 SYNTHESIS

2.1.1 Phosphine ligands

In this study, three phosphine ligands were used as the starting blocks for the preparation of coordination compounds: bis (diphenylphosphinomethyl)-phenylphosphine (**PPP**), tris(diphenyl-phosphinomethyl)phosphine (**PPPP**) and bis-(2-(diphenylphosphino)phenyl phosphine oxide (**P(PO)P**) (Scheme 1).

Scheme 1. Schematic structures of the phosphine ligands **PPP**, **PPPP** and **P(PO)P**.

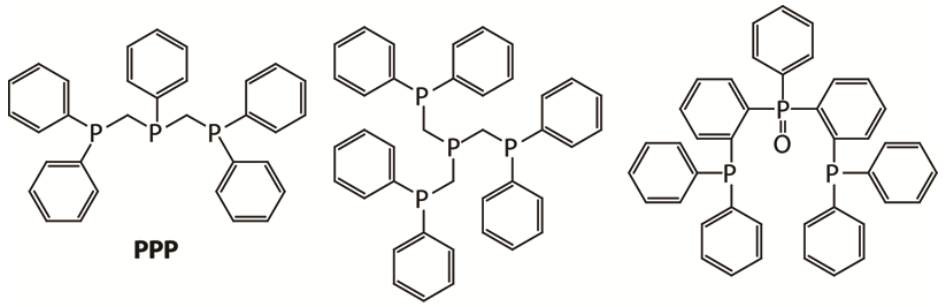

Ligands **PPP** and **PPPP** were synthesized according to the published procedures[48,49] (Scheme 2), the preparation of the new ligand **P(PO)P** is given in section 3.3.

Scheme 2. Synthesis of the ligands **PPP**[48] and **PPPP**[49].

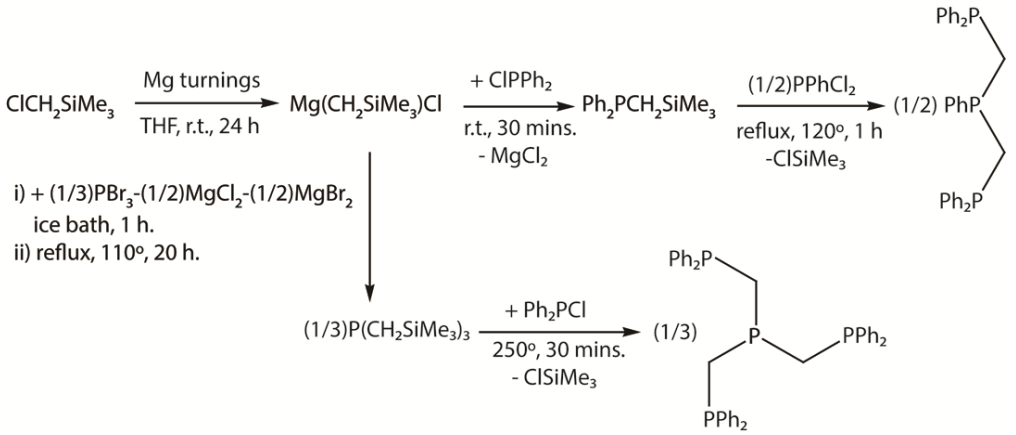

2.1.2 Metal complexes

The phosphine ligands **PPP**, **PPPP** and **P(PO)P** were used to synthesize 30 novel homo- and heterometallic complexes of gold(I), copper(I) and silver(I) (Table 1). The starting compounds $(AuSPh)_n$[50], $(AuC_2R)_n$ (R = Ph, biphenyl, terphenyl, 4-NMe_2-C_6H_4,

4-OMe-C_6H_4, 4-CF_3-C_6H_4, cyclohexanolyl, Fc (ferrocenyl), Fc-C_6H_4)[51] and Au(tht)Cl (tht = tetrahydrothiophene)[52] were prepared according to the published procedures. Complexes **1**−**30** were obtained by following the general methods of coordination and organometallic chemistry. The detailed synthetic procedures are described in publications I–V, and in the discussion of the results in the next chapter.

Table 1. Metal complexes **1**−**30** in this study.

Ligand	Metal core	Ancillary ligand	Complex formula	Publ
	Au_4	-C_2Ph	$[Au_4(C_2Ph)_2(PPP)_2](PF_6)_2$ (**1**)	I
	Au_4	-$C_2C_6H_4Ph$	$[Au_4(C_2C_6H_4Ph)_2(PPP)_2](PF_6)_2$ (**2**)	I
	Au_4	-$C_2(C_6H_4)_2Ph$	$[Au_4(C_2(C_6H_4)_2Ph)_2(PPP)_2](PF_6)_2$ (**3**)	I
	Au_4	-$C_2C_6H_4OMe$	$[Au_4(C_2C_6H_4OMe)_2(PPP)_2](PF_6)_2$ (**4**)	I
	Au_4	-$C_2C_6H_4NMe_2$	$[Au_4(C_2C_6H_4NMe_2)_2(PPP)_2](PF_6)_2$ (**5**)	I
PPP	Au_4	-$C_2C_6H_{10}$(OH)	$[Au_4(C_2C_6H_{11}O)_2(PPP)_2](ClO_4)_2$ (**6**)	I
	Au_4	-$C_2C_6H_4CF_3$	$[Au_4(C_2C_6H_4CF_3)_2(PPP)_2](PF_6)_2$ (**7**)	I
	Au_4	-SPh	$[Au_4(SPh)_2(PPP)_2](PF_6)_2$ (**8**)	I
	Au_4	-C_2Fc	$[Au_4(C_2Fc)_2(PPP)_2](PF_6)_2$ (**9**)	II
	Au_4	-$C_2C_6H_4Fc$	$[Au_4(C_2C_6H_4Fc)_2(PPP)_2](PF_6)_2$ (**10**)	II
PPP	Au_3		$[Au_3(PPP)_2](PF_6)_3$ (**11**).	III
PPP	$AuCu_2$		$[AuCu_2(PPP)_2](PF_6)_3$ (**12**).	III
PPP	$AuAg_2$		$[AuAg_2(PPP)_2](PF_6)_3/(ClO_4)_3$ (**13a**/**13b**)	III
PPPP	Ag_4		$[Ag_4\{(PPPP\}_2](ClO_4)_4$ (**14**)	III
PPPP	Au_4		$[Au_4\{(PPPP\}_2](PF_6)_4$ (**15**)	III
PPPP	$AuAg_3$		$[AuAg_3\{(PPPP\}_2](ClO_4)_4$ (**16**)	III
PPPP	Au_2Cu_2		$[Au_2Cu_2\{(PPPP\}_2(NCMe)_2](PF_6)_4$ (**17**)	III
	Cu		CuCl(P(PO)P) (**18**)	IV
	Cu		CuBr(P(PO)P) (**19**)	IV
	Cu		CuI(P(PO)P) (**20**)	IV
	Ag		AgCl(P(PO)P) (**21**)	IV
	Ag		AgBr(P(PO)P) (**22**)	IV
	Ag		AgI(P(PO)P) (**23**)	IV
P(PO)P	Cu_2		$[Cu(P(PO)P)]_2(PF_6)_2$ (**24**)	IV
	Ag_2		$[Ag(P(PO)P)]_2(CF_3SO_3)_2$ (**25**)	IV
	Au_2		$[Au(P(PO)P)]_2(PF_6)_2$ (**26**)	IV
	AuCu		$[AuCu(P(PO)P)]_2(PF_6)_2$ (**27**)	IV
	$AuCu_2$		$[(P(PO)P)_2AuCu_2(C_2C(OH)Ph_2)_2]CF_3SO_3$ (**28**)	V
	$AuAg_2$		$[(P(PO)P)_2AuAg_2(C_2C(OH)Ph_2)_2]CF_3SO_3$ (**29**)	V
	$AuAg_2$		$[(P(PO)P)_2AuAg_2(C_2Ph)_2]CF_3SO_3$ (**30**)	V

2.2 CHARACTERIZATION

Slow evaporation or vapor diffusion techniques were used to recrystallize the complexes **1**−**30**. The solid-state structures were determined by single crystal X-ray crystallography (XRD) and the purity of the bulk samples was confirmed by elemental analysis. ^{1}H, $^{31}P\{^{1}H\}$, and $^{1}H-^{1}H$ COSY NMR spectroscopy and electrospray ionization mass spectrometry (ESI-MS) were used to investigate these complexes in solution.

The photophysical measurements and the computational analysis of the electronic structures were performed by collaborative groups at the National Taiwan University (Taiwan, Prof. Pi-Tai Chou), St. Petersburg State University (Russia, Prof. Sergey P. Tunik) and Aalto University (Finland, Prof. Antti J. Karttunen). The author has analysed these data.

3 RESULTS AND DISCUSSION

3.1 TETRAGOLD(I) COMPLEXES BASED ON THE TRIPHOSPHINE (PPP) LIGAND

Despite significant progress in the study of gold chemistry, the gold(I)-only molecular clusters have been poorly explored in respect to their photophysical performance dependent upon the properties of ancillary ligands (alkynes, thiols, aryl groups).[47d,53] In this work, a family of triphosphine-supported tetragold(I) clusters was prepared by incorporating the alkynyl and thiolate ancillary ligands, which provided a convenient opportunity for the systematic alteration of the electronic properties of the ligand sphere, and thus allowed one to investigate the influence of the ancillary ligands on the structural and optical features.

3.1.1 Alkynyl and thiolate tetragold(I) complexes based on the triphosphine PPP ligand.

The starting cationic precursor $[Au_3(\mathbf{PPP})_2]^{3+}$ was obtained by reacting $AgPF_6/AgClO_4$ with a stoichiometric mixture of AuCl(tht) and a **PPP** ligand. Then, treatment of the intermediate gold complexes (**PPP**)$(AuC_2R)_3$ and (**PPP**)$(AuSPh)_3$, which were generated by depolymerization of the compounds $(AuC_2R)_n$ and $(AuSPh)_n$, respectively, with a stoichiometric amount of $[Au_3(\mathbf{PPP})_2]^{3+}$ produced the tetranuclear clusters $[Au_4(\mathbf{PPP})_2(C_2R)_2]^{2+}$ (R = Ph (**1**), biphenyl (**2**), terphenyl (**3**), C_6H_4OMe (**4**), $C_6H_4NMe_2$ (**5**), $C_6H_{11}O$ (**6**), $C_6H_4CF_3$ (**7**), Fc (**9**), C_6H_4Fc (**10**)) and $[Au_4(\mathbf{PPP})_2(SPh)_2]^{2+}$ (**8**), which were isolated in high yields as moisture and air-stable solids after crystallization (Scheme 3).

Scheme 3. Synthesis of clusters **1**−**10** (dichloromethane, 298 K, 1 hour, 79–96%).

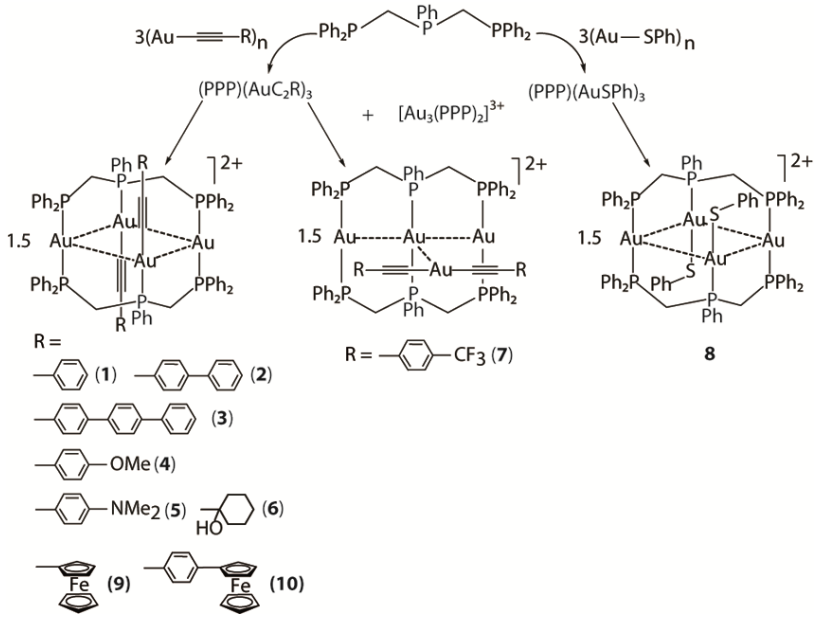

According to the XRD structural investigations, all clusters of this series adopt the rhomboidal {Au_4} core bridged by two bent **PPP** ligands, except complex **7** bearing –C≡C–$C_6H_4CF_3$ group, which shows a T-like arrangement of the metal framework. The aurophilic interactions evidently stabilize the tetrametallic motif, while phosphine ligands largely determine its geometry.

In complexes **1**−**6** and **8**−**10**, the Au–Au bond lengths lie in the range of 3.0368(1)−3.2325(3) Å, these values are typical for effective gold-gold contacts.[22a,54] The rhomboidal motif of these clusters (Fig. 12) is similar to that of the triphosphine-chloride gold(I) compound [Au_4(**PPP**)$_2Cl_2$](CF_3SO_3)$_2$ reported by Laguna and co-workers.[55] However, the Au–P distances in this dichloride congener are slightly different from those in **1**−**6** and **8**−**10,** apparently due to the variation of the nature of ancillary ligands.

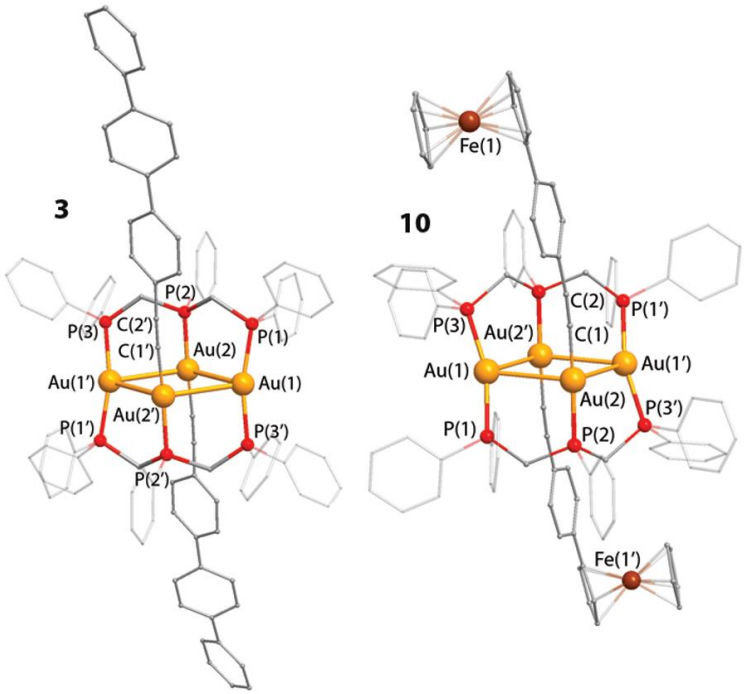

Figure 12. Molecular views of dications **3** and **10**.

The alkynyl (**1**−**6**, **9**−**10**) and thiolate (**8**) groups are connected to the corresponding gold centers in η^1-mode, which implies no interactions between the π-systems of the –C≡C– moieties and the adjacent metal ions. The structural parameters of clusters **1**−**6** and **8**−**10** and the electronic properties of the alkynyl/thiolate substituents display no systematic correlations.

In **7**, a T-like arrangement of the metal core features the linear trimetallic fragment [Au_3(**PPP**)$_2$]$^{3+}$ coupled with a gold dialkynyl anion *via* the unsupported Au(2)−Au(3) bond (3.0092(3) Å) , Fig. 13. A similar T-shaped motif has been also found in heterometallic Au_2Ag_2 alkynyl complexes.[41] The metal core of **7** possesses a slightly longer

Au(1)–Au(2) distance (2.9855(2) Å) and a distorted linear chain Au(1)–Au(2)–Au(1') (angle 169.9º) in comparison to the corresponding values in the parent compound $[Au_3(\mathbf{PPP})_2]^{3+}$ (2.9243(2) Å and 180º, see section 3.2). The nearly linear angle C(1)–Au(3)–C(1´) of 176.2º indicates that the typical coordination geometry of the $[Au(C_2C_6H_4CF_3)_2]^-$ unit is retained in dication **7**. Interestingly, the aurophilic bonds in **7** lie in the range of 2.9855(2)–3.0092(3) Å, which are shorter than those in rhomboidal structures **1**−**6** and **8**−**10**. In addition, similarly to **1**−**6** and **8**−**10**, no substantial η^2 interactions are to be found between the -C≡C- units of the alkynyl ligands and adjacent metals centers (Au(1) and Au(1´)) in **7**.

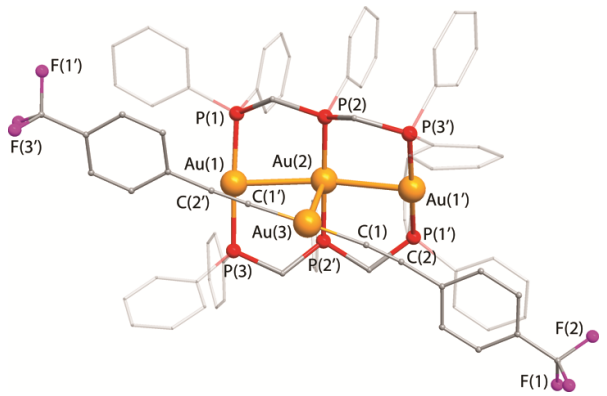

Figure 13. Molecular view of dication **7**.

It is assumed that the subtle electronic factors govern the unique T-like arrangement of metal core in complex **7,** as it was found only in the case of an electron-withdrawing alkynyl substituent (CF_3) in the absence of obvious steric hindrances. Unfortunately, no cluster could be obtained using an electronically similar ligand $–C≡C–C_6H_4NO_2$ to confirm this hypothesis.

The NMR and ESI-MS spectroscopic measurements confirm that these complexes (**1**−**10**) retain their compositions in solution. However, in a fluid medium, compounds **1**−**7** exist as two isomers (forms **I** and **II**) being in slow chemical equilibria (Scheme 4).

Scheme 4. Proposed interconversion of the isomeric forms of **1**–**7**.

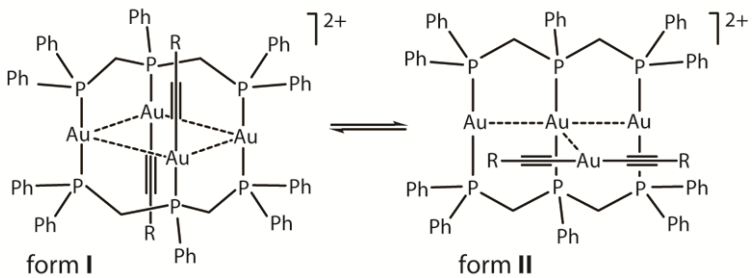

The rhomboidal structural motif found in clusters **1**–**6** corresponds to form **I**, and the T-shape framework of complex **7** is assigned to form **II.** Additionally, no appreciable isomerization was revealed for the ferrocenyl alkynyl complexes **9** and **10** that can be tentatively explained by the presence of bulky Fc groups on the alkynyl ligands, which might sterically prevent the appearance of form **II**. For instance, an equilibrium between two isomeric structures is clearly visible in the solution of **7** (Fig. 14). Both forms of this cluster display the A_4B_2 patterns in the $^{31}P\{^1H\}$ NMR spectrum. Based on the spin system simulation, one isomer is assigned to form **I** and reveals two multiplets at 22 and 40 ppm, which are typically observed in the spectra of the freshly prepared solutions of rhomboidal clusters **1**–**6** and **9**–**10**. Consequently, two other signals at 26 and 31 ppm can be attributed to the T-shaped isomer (form **II)**.

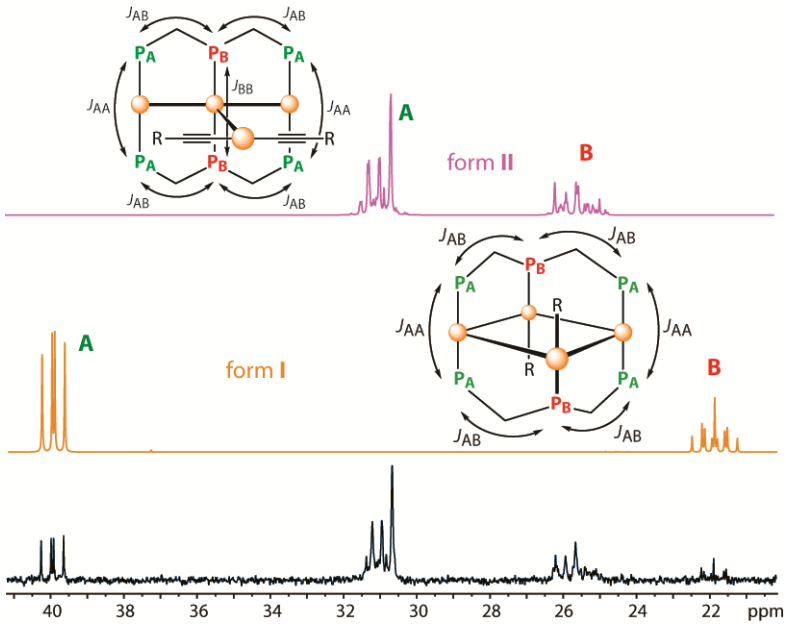

Figure 14. ^{31}P NMR spectrum of an equilibrated solution of 7, acetone-d_6, 298 K (bottom). Simulation of A_4B_2 systems: form I J_{AA} = 320 Hz, J_{AB} = 75 Hz (top, orange); form II J_{AA} = 310 Hz, J_{BB} = 310 Hz, J_{AB} = 74 Hz (top, purple).

The photophysical properties of complexes **1**−**8** were mainly studied in the solid state due to the low intensity of the emission in solution and the isomerization mentioned above. These compounds display moderate to strong phosphorescence with a wide variation of the emission energy ranging from 443 to 615 nm. The quantum efficiencies at room temperature reach a good value of 51% (**5**, Table 2). It is worth mentioning that complex **1** exhibits double-exponential decay (2 distinctive lifetimes, 7.54 and 11.74 μs) with two emission bands at 440 nm and 650 nm, which were tentatively assigned to the change in the crystalline phases due to the loss of the crystallization solvent. Other clusters **2**−**8** show single emission bands with emission lifetimes in the microsecond domain (0.88−18.10 μs).

Table 2. Photophysical properties of complexes **1**–**8** and Laguna's compound $[Au_4(PPP)_2Cl_2][CF_3SO_3]$ at room temperature.

	λ_{ab}/ nm[a]	λ_{em}/ nm[b]	Φ[b], %	τ_{obs}/μs
Au_4Cl_2[55]	~295	~515[b]		
1	308	440, 650	26	7.54 (440 nm), 11.74 (650 nm)
2	350	520	15	18.10
3	361	543	9	16.30
4	354	460	44	7.59
5	414	573	51	1.94
6	300	530	30	4.51
7	348	477	22	5.06
8	393	615	7	0.88

[a] solution; [b] solid.

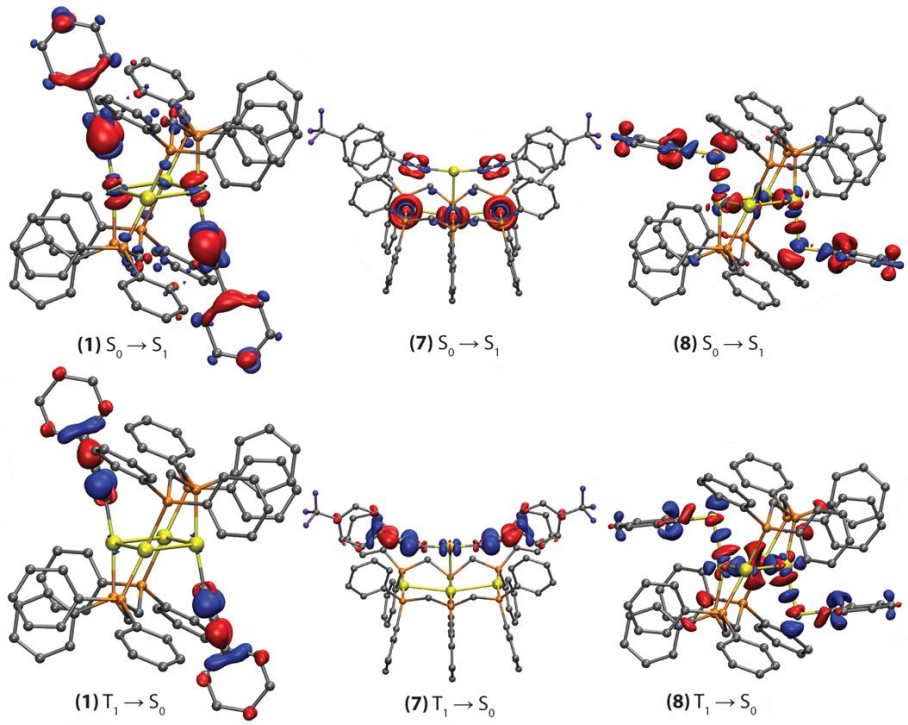

Figure 15. Electron density difference plots for the lowest energy singlet excitation ($S_0 \rightarrow S_1$) and the lowest energy triplet emission ($T_1 \rightarrow S_0$) of the Au(I) clusters **1**, **7** and **8** (isovalue 0.002 a.u.). The electron density increases in the blue areas and decreases in the red areas, during the electronic transition.

The emission can be tuned by altering the electron-donating properties of the alkyne ligands in these alkynyl tetragold(I) complexes. However, in the solid state, the correlation might not be as smooth as expected. Thus, complex **4** with its electron-rich alkyne ($–C_2C_6H_4OMe$) behaves as an outlier. Nevertheless, a crude correlation might be seen, which is generally in line with other examples[56], where a decrease of emission energy upon the increase of the electron donating ability of the alkynyl ligands is normally observed.

DFT calculations support the experimental studies and demonstrate the important role of Au atoms, with variable contributions of the alkyne and thiolate ligands in the excitation and emission properties of complexes **1**–**8** (Fig. 15).

Due to the high photoluminescence intensity in the solid (Φ = 0.51), complex $[Au_4(C_2C_6H_4NMe_2)_2(PPP)_2](PF_6)_2$ (**5**) was employed as an emitter to fabricate an OLED device, which reached good quantum efficiency for the first time with polynuclear Au(I) complexes. The diode shows a high maximum brightness of 7430 cd/m^2 at 10 V. The highest external quantum efficiency was 3.1%, which in terms of power and current efficiencies gives the values of 5.3 lm/W and 6.1 cd/A, respectively (Fig. 16).

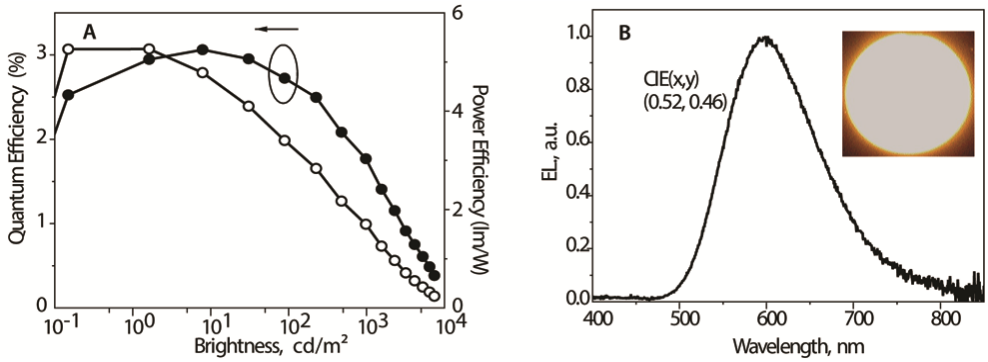

Figure 16. (A) External quantum and power efficiencies as a function of brightness; (B) normalized EL spectrum of the device with compound **5** as the dopant.

For comparison, it should be noted that earlier very few EL devices using gold(I) complexes were described. For example, the OLEDs with $[Au(4\text{-}R\text{-}dppn)_2]X$ (dppn = 1,8-bis(diphenylphosphino)naphthalene; R = H, Me) or $[Au_2(dppm)_2]^{2+}$ (dppm = bis(diphenylphosphino)methane as triplet emitters were reported to exhibit very low quantum efficiencies (< 0.1-0.02%).[57] Although the OLED performance in the current work has not been fully optimized, its good efficiency and solution processability demonstrate a promising concept for employing phosphorescent metal clusters as emitters in electroluminescent devices. Lately, Chen et al. have further developed this approach and reported high-efficiency EL devices with polynuclear complexes (Au_4Ag_2 and $PtAu_2$ phosphine-alkynyl clusters) as having maximum external quantum efficiencies (EQE) of 7.0% and 21.5%, respectively.[42c,58]

3.1.2 Ferrocenyl tetragold(I) complexes based on the triphosphine (PPP) ligand

As shown above, ancillary alkynyl ligands have a significant influence on the physical characteristics of the gold(I) compounds. As a continuation of the studies of the tetragold(I) species, ferrocenyl units (Fc) were introduced as end-capping moieties of the alkynyl groups in **9** and **10**. The presence of terminal redox active functions allows one to explore the possibility of electronic communication through the conjugated chain of the molecular wire[59] and to evaluate the ability of Au_4 metal core to act as a junction between the Fc groups. In order to fulfil this aim, cyclic voltammetry (CV) and square wave voltammetry (SWV) were used to study the electrochemical behaviour of Fc-funtionalized clusters **9** and **10** (Fig. 17).

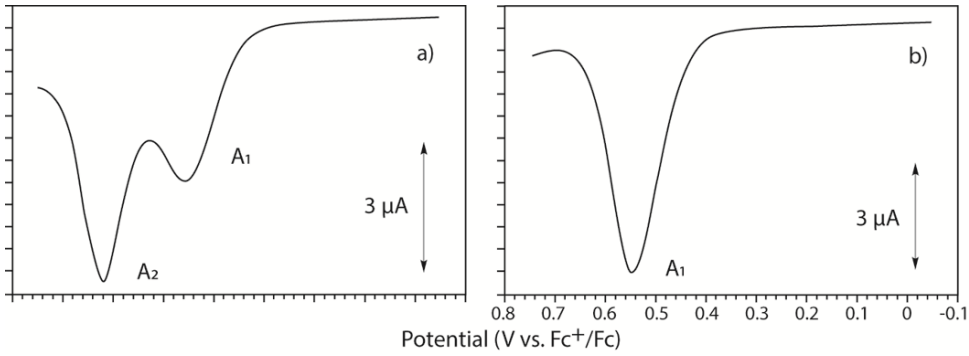

Figure 17. Square wave (SW) voltammograms at a glassy carbon electrode for *ca.* 1 mM solutions of: a) **9**, b) **10**, in 0.10 M Bu_4NPF_6. Potential scan initiated at –0.05 V in the positive direction. Potential step increment 4 mV; SW amplitude 25 mV; frequency 5 Hz.

The results of the electrochemical measurements indicate the redox processes in clusters **9** and **10**, which are assigned to the reversible oxidation of the end-capped ferrocenyl moieties. The squarewave voltammogram in **9** displays two peaks, which points to an electron transfer between the Fc units. The {Au_4} metal core, in this case, provides good conjugation and mediates efficient charge mobility. In **10**, however, no electronic communication between redox sites is found based on their essentially independent behaviour.

It is worth comparing the observed behaviour of **9** with related examples. Zanello and co-workers reported no electronic transfer between two ethynyl-ferrocene functions mediated by a metal core {Pt_6}.[60] Moreover, the {Au_4} core in **9** provides more effective Fc–Fc coupling even than that in a directly linked system Fc-C≡C-C≡C-Fc[61] that is reflected by the higher peak potential separation ΔE (0.14 V vs < 0.135 V) observed in **9**. This is an unexpected feature because two Fc-C≡C- fragments in **9** do not constitute a rodlike conjugated structure. Therefore, the tetragold framework is a potentially effective electronic mediator, which can serve as a promising candidate for an electronic connection in switchable molecular devices.

3.2 COINAGE METAL COMPLEXES BASED ON TRI- AND TETRA-PHOSPHINE (PPP AND PPPP) LIGANDS

Altering the electronic features of the ligand sphere offers a facile way to tune the optical properties of the polynuclear d^{10} metal clusters.[56] Apart from the ligands, metal-metal interactions, which are typically found among the coinage metal ions, have also displayed significant influence on the photophysics of d^{10}-metal based materials.[9,38,62,63] To minimize the influence of ancillary ligands, further work aimed at studying the effect of the composition and geometry of the metal framework on the luminescence behaviour of the homoleptic polymetallic assemblies, supported by the tri- and tetradentate phosphines **PPP** and **PPPP**.

3.2.1 Trinuclear PPP complexes.

Complex $[Au_3(\mathbf{PPP})_2]^{3+}$ (**11**) was synthesized by a modified procedure reported by Che (Scheme 5).[27] Alternatively, treatment of the AuCl(tht) (tht = tetrahydrothiophene) precursor with a stoichiometric amount of the **PPP** triphosphine followed by the exchange of chloride anions with $AgPF_6$ and addition of two equivalents of M^+ cations as PF_6^- salts afford heterometallic trinuclear clusters of a general composition $[AuM_2(\mathbf{PPP})_2]^+$ (M = Cu (**12**), Ag (**13**) (Scheme 5).

Scheme 5. Syntheses of clusters **11**−**13**.

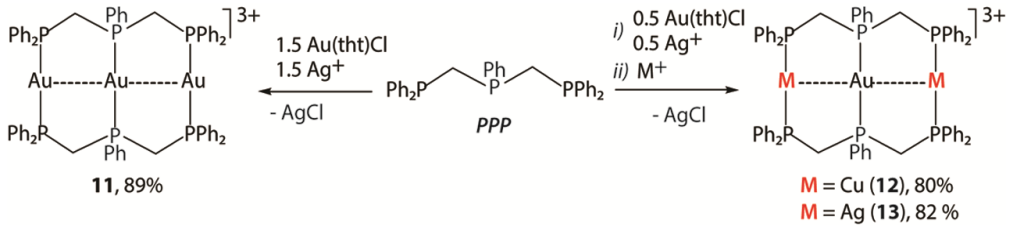

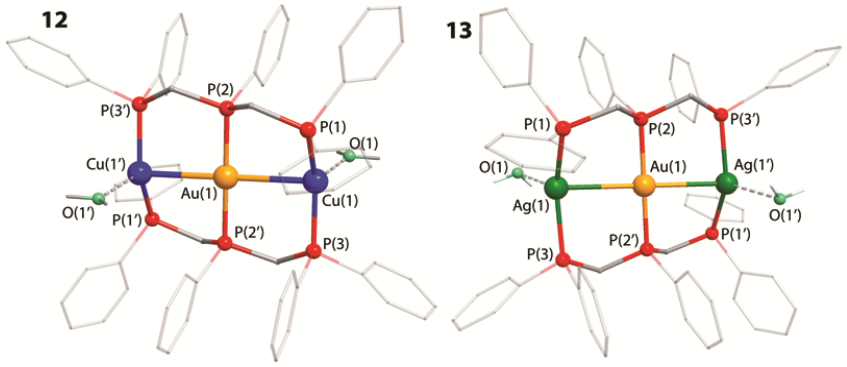

Figure 18. Molecular views of trications **12** and **13**.

According to the XRD data, complexes **11**–**13** possess linear metal frameworks (M(1)−Au(2)−M(1′) angles equal 180°), which are held together by two bridging **PPP** ligands (Fig. 18). Both heterometallic species **12** and **13** have water molecules weakly

bound to Cu and Ag atoms, respectively, that reflects their tendency to have a higher coordination number than the Au(I) ions.

The detailed NMR spectroscopic investigation shows that the homometallic cluster **11** retains its structure in solution. On the contrary, heterometallic compounds **12** and **13** reveal the redistribution of the metal ions accompanied by reversible solvation-desolvation to produce the mixtures of the trimetallic species, which, however, selectively crystallize in the forms of **12** and **13**. For example, three groups of signals, which arise from the complicated exchange dynamics, can be identified in the ^{31}P–^{31}P COSY NMR spectrum of **13** in DMSO-d_6 (Fig. 19).

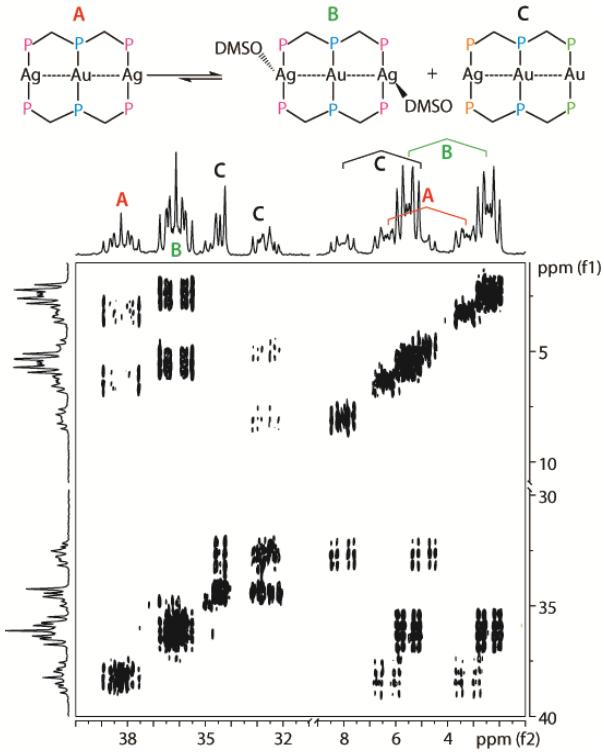

Figure 19. Proposed solvate forms equilibrium in **13** (top), and ^{31}P-^{31}P COSY NMR spectrum of **13**, DMSO-d_6, 298 K (bottom).

By using spin simulation, two groups are tentatively assigned to the symmetrical solvent-free (**A**) and DMSO solvated (**B**) $[AuAg_2(\mathbf{PPP})_2]^{3+}$ ions, and the third group arises from the asymmetric $[Au_2Ag(\mathbf{PPP})_2]^{3+}$ species (**C**). In **C**, two resonances in the low field (34.4 ppm, 32.7 ppm) correspond to the Au-coordinated phosphorus atoms, while the high-field one at 6.4 ppm displays a typical coupling pattern of ^{31}P to $^{107/109}Ag$. A probable formation of the trisilver complex $[Ag_3(\mathbf{PPP})_2]^{3+}$ and of its solvated derivatives may support the appearance of the latter species **C** to compensate for the stereochemistry of the system. However, these proposed compounds of the brutto composition $[Ag_3(\mathbf{PPP})_2]^{3+}$ are not detected in the ^{31}P–^{31}P NMR spectrum,

probably due to their relatively low concentration and their involvemet in a number of dynamic processes.

The photophysical properties of clusters **11**−**13** were studied only in the solid state, because of their stereochemical non-rigidity in solution. Complexes **11**−**13** exhibit moderate to strong phosphorescence (quantum yields 20-64%***)*** with lifetimes in the microsecond domain (Table 3). It is worth mentioning that the pure gold content in the cluster core (**11**) gives the highest quantum effiency (Φ =64% in KBr tablet and 90% in the neat crystalline form).

Table 3. Photophysical properties of **11**–**13** in solid state, 298 K.

	λ_{ex}, nm	λ_{em}, nm	τ_{obs}, μs	Φ, %
11	330 sh, 365, 400 sh	460	2.4 ± 0.1	64
12	340sh, 380	515	19.3 ± 0.2	30
13	315sh, 380	450	2.0 ± 0.2 (0.72), 0.6 ± 0.1(1.0)	20

The TD-DFT calculations confirm the experimental values (Fig. 20) and show that the radiative $T_1 \rightarrow S_0$ transitions in **11**−**13** clearly have a metal-centered origin, with only a small contributions from the phosphines.

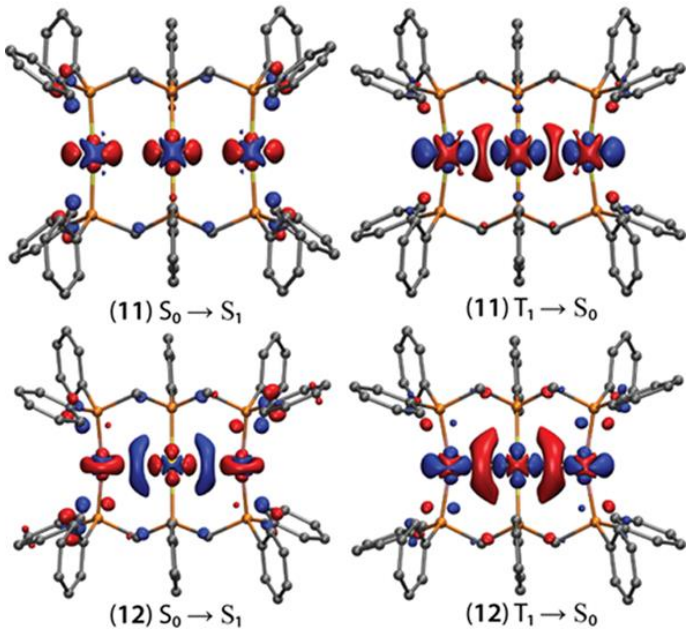

Figure 20. Electron density difference plots for the lowest energy singlet excitation ($S_0 \rightarrow S_1$) and the lowest energy triplet emission ($T_1 \rightarrow S_0$) of clusters **11** and **12** (isovalue 0.002 a.u.). During the electronic transition, the electron density increases in the blue areas and decreases in the red areas.

3.2.2 Tetrametallic PPPP complexes

To extend the investigation of the influence of the metal core on the photophysical properties, tetraphosphine **PPPP** ligand was used to prepare the series of tetranuclear compounds.

The homometallic species $[M_4(\mathbf{PPPP})_2]^{4+}$, M = Ag (**14**), Au (**15**) were synthesized by reacting $AgClO_4$ (**14**) or AuCl(tht) in the presence of Ag^+ (**15**) with a 0.5 equivalent of **PPPP** (Scheme 6).

Consecutive addition of Au^+ (which are produced *in situ* by removal of the chloride from Au(tht)Cl with Ag^+ in the presence of an excess of tht) and Ag^+ ions to the tetradentate phosphine resulted in the formation of the heterometallic complex $[AuAg_3(\mathbf{PPPP})_2]^{4+}$ (**16**) that features the same structural motif as that of **14** and **15**. However, following this pathway in an attempt to generate similar tetranuclear Au−Cu cluster, the complex of a different structural type $[Au_2Cu_2(\mathbf{PPPP})_2(NCMe)_4]^{4+}$ (**17**, Scheme 6) was isolated; using the proper stoichiometry resulted in a good yield of the reaction.

Scheme 6. Syntheses of the clusters **14**−**17.**

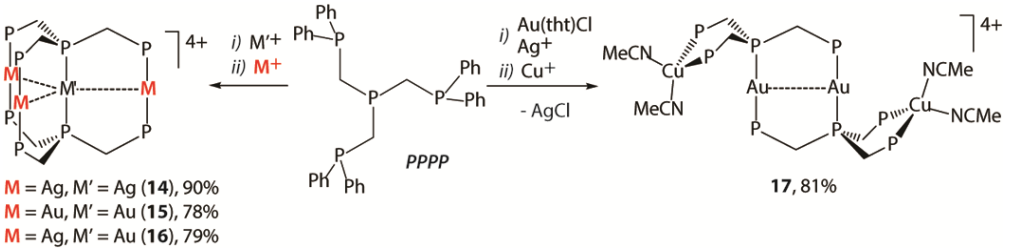

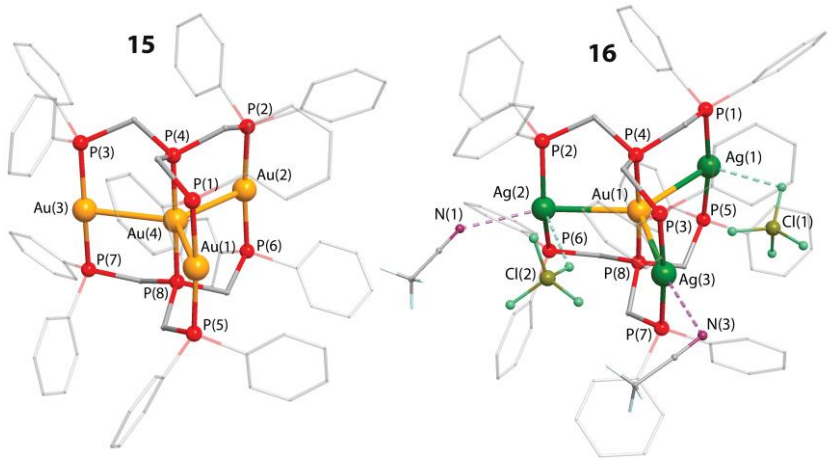

Figure 21. Molecular views of the tetracations **15** and **16**. The counterions and acetonitrile molecules bound to the metal ions are shown for **16**.

In clusters **14**–**16** (Fig. 21), the metal atoms form approximately planar star-shaped cores, with one metal ion in the middle and three others located in the corners of an equilateral triangle.

The values of the metal-metal distances are typical for the d^{10} metallophilic interactions (Ag–Ag, Au–Au and Ag–Au) reported in literature.[2c,22a,27,64] This metal-metal bonding together with the stereochemistry of the **PPPP** ligands determines the given arrangement of metal ions in complexes **14**–**16**. The ClO_4^- salts of Ag-containing compounds **14** and **16** are isomorphic and have weakly coordinated acetonitrile ligands, which can be easily removed upon vacuum drying to give solvent-free materials.

The Au–Cu complex **17** features a different structural motif than that of **14**–**16**. In **17** a digold unit is bridged by two arms of the equivalent **PPPP** ligands and the Cu^I ions are chelated by the remaining phosphorus atoms of each tetraphosphine (Fig. 22). The tetrahedral coordination geometry around the copper atoms is completed by the additional binding of two acetonitrile molecules. No Au−Cu interactions are found due to the long distances between gold and copper ions, which exceed 4.7 Å.

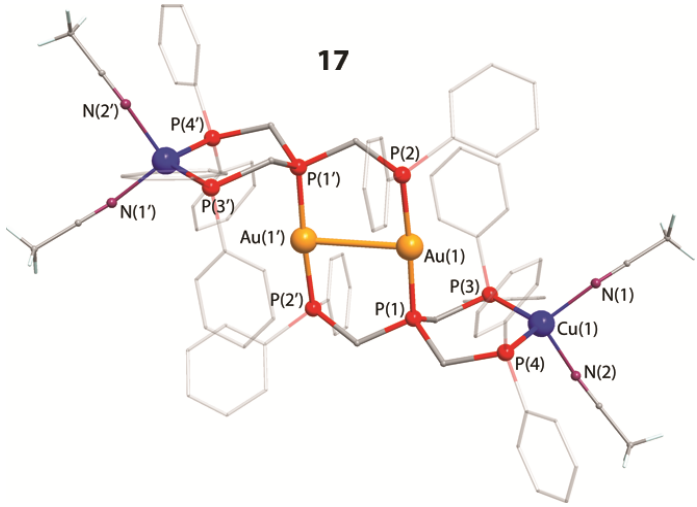

Figure 22. Molecular view of tetracation **17**.

The NMR spectroscopic measurements show that clusters **14**, **15** and **17** retain their structures in solution and display the spectroscopic patterns, which correspond to the idealized molecules of C_{3h} and C_i symmetry point groups, respectively. The Au–Ag heterometallic complex **16** demonstrates exchange dynamic behavior in DMSO solution, which involves the redistribution of the metal ions and leads to the appearance of at least two novel species (Fig. 23); the process is similar to that described above for **13**.

As for trimetallic compounds **11**–**13**, the photophysical behaviour of clusters **15**−**17** was studied only in solid state, while the homonuclear silver complex **14** is nonemissive both in solution and in neat powder. Its gold relative (**15**) shows relatively

strong luminescence (Φ_{em} 30%); both components of double exponential decay (6.4 and 3.0 μs) point to the triplet origin of emission (Table 4). The heteronuclear {$AuAg_3$} analogue **16** also shows an emission energy similar to that of **15** but with a visibly smaller quantum yield (16%). Taking into account the isomorphism of complexes **14** and **16**, their distinctive photophysical properties can be attributed to the difference in the compositions of the metal cores ({Ag_4} vs {$AuAg_3$}).

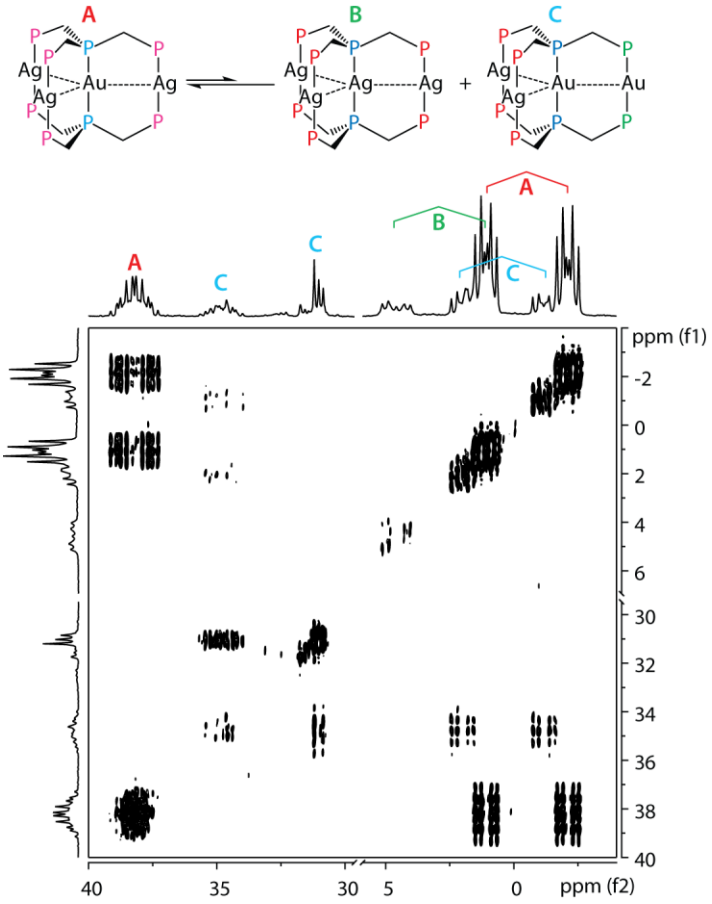

Figure 23. Proposed migration of the metal ions in **16** (top), and the ^{31}P-^{31}P COSY spectrum of **16**, DMSO-d_6, 298 K (bottom). The low-field signal of **14** (B) at 14.9 ppm has been omitted for sake of clarity.

A significant red shift of emission maximum is observed for complex **17** (λ_{em} = 563 nm, lifetimes of 0.7 and 0.4 μs, Φ_{em} 6%) compared to the **11**−**13**, **15**, and **16** series. The presence of two components in the emission decay of **13**, **15**−**17** can be related to the disorder of the nearest environment of the metal core, which may originate from the (*i*) presence of a weakly coordinated crystallization solvent, and/or (*ii*) alterations in the arrangement of the weakly bound counterions around the cationic cluster. These two features may activate two different relaxation pathways of the excited state.

According to TD-DFT calculations, the $T_1 \rightarrow S_0$ transitions in clusters **15** and **16** are mostly assigned to metal-centered parentage mixed with some contributions from the phosphines (Fig. 24). On the other hand, the lowest energy triplet to singlet relaxation ($T_1 \rightarrow S_0$) in **17** is rather delocalized over the whole molecule (Fig. 24).

Table 4. Photophysical properties of **15**–**17** in solid state, 298 K[a].

	λ_{ex}, nm	λ_{em}, nm	τ_{obs}, μs	Φ, %
15	330sh 390	460, 550sh	6.4 ± 0.2 (0.62), 3.0 ± 0.1 (1.0)	30
16	340sh, 365	450	1.8 ± 0.2 (0.46), 0.6 ± 0.1(1.0)	16
17	335, 365	563	0.7 ± 0.1(0.75), 0.4 ± 0.1 (1.0)	6

[a] Relative contribution of each exponent into double exponential decays are given in parentheses.

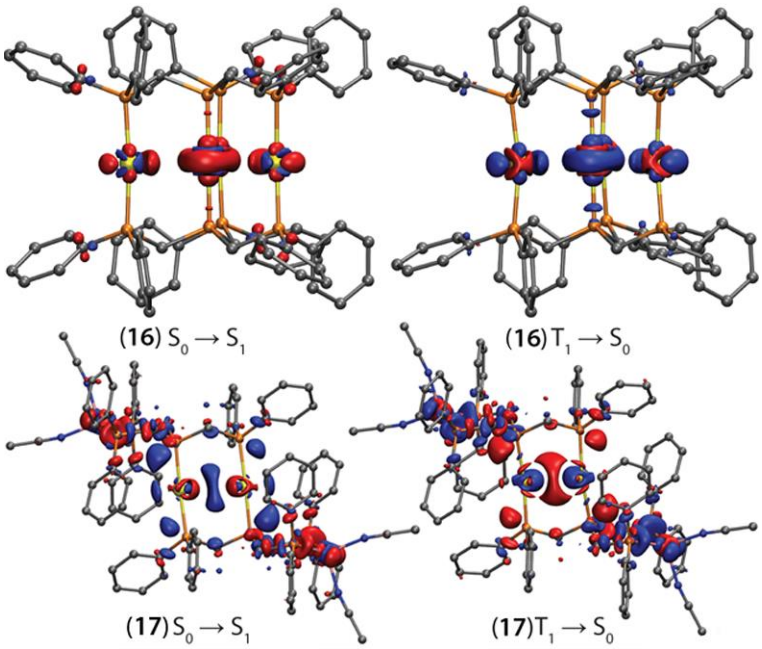

Figure 24. Electron density difference plots for the lowest energy singlet excitation ($S_0 \rightarrow S_1$) and the lowest energy triplet emission ($T_1 \rightarrow S_0$) of clusters **16** and **17** (isovalue 0.002 a.u.). During the electronic transition, the electron density increases in the blue areas and decreases in the red areas.

3.3 COINAGE METAL COMPLEXES BASED ON A HYBRID PHOSPHINE–PHOSPHINE OXIDE (P(PO)P) LIGAND

Hemilabile phosphine ligands containing both strong and weak binding moieties have been extensively utilized in various catalytic applications[65,66], as molecular chemosensors[67], and for the construction of functional supramolecular complexes through a weak-link approach.[68] The studies of the heterodentate P-PO (phosphine–phosphine oxide) ligands remain quite limited among the family of hemilabile compounds. Moreover, these mixed P-PO ligands have not been used for the design of luminescent transition metal complexes. Therefore, in the current research, we aimed at investigating the possible effect of the hemilabile coordination of a hybrid P-PO ligand on the molecular assembly of the coinage-metal complexes and their photophysical performance.

An attempt to synthesize a P-PO derivative of bis(diphenylphosphinomethyl)-phenylphosphine (**PPP**), studied earlier, was unsuccessful. Therefore, the mixed bis-(2-(diphenylphosphino)phenyl phosphine oxide (**P(PO)P**) containing aromatic spacers was prepared in good yield (Scheme 7).

Scheme 7. Synthesis of the hybrid ligand **P(PO)P**.

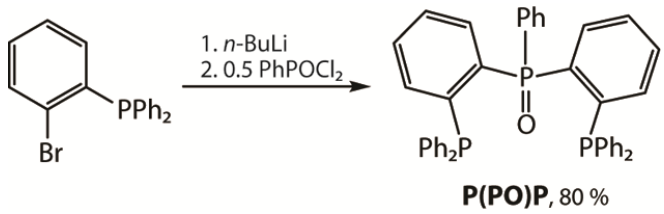

3.3.1 Mono- and dinuclear P(PO)P complexes

Mononuclear halide complexes M(P(PO)P)X. The copper(I) complexes Cu(**P(PO)P**)X, X = Cl (**18**), Br (**19**), I (**20**) were easily formed in the reactions of the copper halides with a stoichiometric amount of a **P(PO)P** ligand (see Scheme 8). An alternative protocol, which involves coupling the **P(PO)P** with $AgPF_6$ and treatment the mixture with the respective NBu_4X salt was followed for the preparation of Ag(**P(PO)P**)X relatives, X = Cl (**21**), Br (**22**), I (**23**) (Scheme 8).

Scheme 8. Synthesis of complexes **18**–**27**.

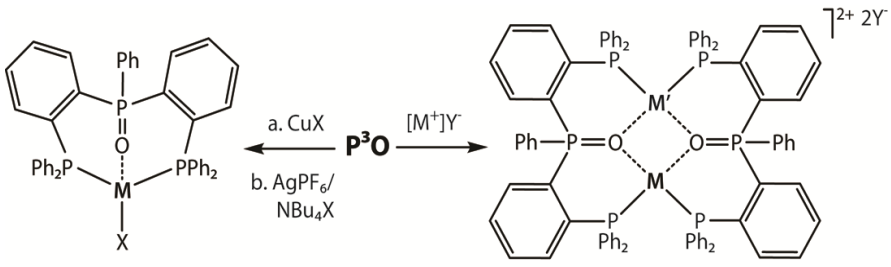

M = Cu, X = Cl, 92% (**18**)
X = Br, 89% (**19**)
X = I, 90% (**20**)
M = Ag, X = Cl, 71% (**21**)
X = Br, 86% (**22**)
X = I, 78% (**23**)

M = M′ = Cu, Y^- = PF_6^-, 90% (**24**)
M = M′ = Ag, Y^- = $CF_3SO_3^-$, 76% (**25**)
M = M′ = Au, Y^- = PF_6^-, 72% (**26**)
M = Au, M′ = Cu, Y^- = PF_6^-, 84% (**27**)

A pseudo-tetracoordinate geometry of the metal ions in **18**–**23** features weak metal–O=P interactions along with the regular metal–phosphine/halide bonding[69] (Fig. 25). The trigonal planar geometry of the MP_2X motif resembles the close relative Ag(*i*-Pr-P(O)P)X[70], and is evidently determined by inefficient coordination of the phosphine oxide function with Cu/Ag ions.

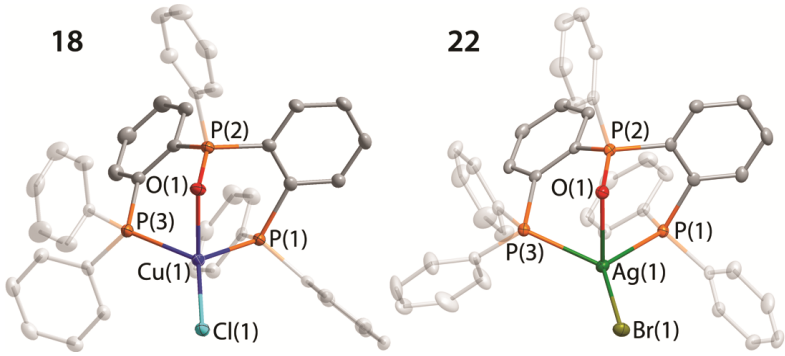

Figure 25. Molecular view of complex **18** and **22**. Thermal ellipsoids are shown at the 50% probability level.

The solution NMR spectroscopic data for the halide complexes **18**–**23** are compatible with their solid state structures. Thus, their $^{31}P\{^1H\}$ spectra show two signals with a 1:2 ratio of integral intensities, corresponding to the P-oxide part and the equivalent metal-bound PPh_2 groups, respectively.

Due to negligible luminescence in solution, the photophysical behaviour of these clusters **18**–**23** was evaluated for the solid samples only. The copper complexes **18** and **19** are not luminescent both at 298 K and 77 K. The iodine complex **20** displays weak orange emission (621 nm, Φ_{em} 0.8%, Table 5), the wavelength of which is nearly temperature insensitive (624 nm at 77 K). Silver complexes Ag(**P(PO)P**)X (**21**–**23**, Table 5) show broad emission bands in a blue region (467–488 nm, Φ_{em} 7.5–20.4%) at

298 K, which are also only slightly altered upon decreasing the temperature to 77 K (464-495 nm).

Table 5. Solid State Photophysical Properties of **20**−**23**.

	λ_{ex}, nm		λ_{em}, nm		τ_{obs}, μs[a]		Φ_{em}, %
	298 K	77 K	298 K	77 K	298 K	77 K	298 K
20	394	362, 380	621	624	0.5	30.7	0.8
21	310, 372	340	480	495	64.8	482.0	17.7
22	362	340	467	464	19.0	529.9	7.5
23	362	353	488	486	38.1	95.7	20.4

By comparing the M(**P(PO)P**)Hal species with their triphosphine congeners M(**P(P)P**)Hal, the effect of partial ligand oxidation on the optical behaviours can be revealed. The phosphine-oxide group in the copper complexes causes a very large decrease of quantum yield. Conversely, in the case of the silver complexes the detrimental influence of the **P(PO)P** ligand on the emission intensity is less pronounced. Interestingly, the hybrid phosphine produces a substantial blue shift of the emission maxima. This effect illustrates a facile approach to tune luminescence characteristics of this sort of silver species through a minor ligand modification.

The photophysical behaviour for **20**–**23** has been rationalized by comparing the singly occupied molecular orbitals (SOMO and HSOMO) with the HOMO of the S_0 ground state by the use of DFT calculations. The emission of these mononuclear complexes can be assigned primarily to the MXLCT excited state, and the variations in the metal-ligand interactions between the families containing **P(PO)P** and **P(P)P** phosphines are essentially responsible for the differences in their luminescence properties (Fig. 26).

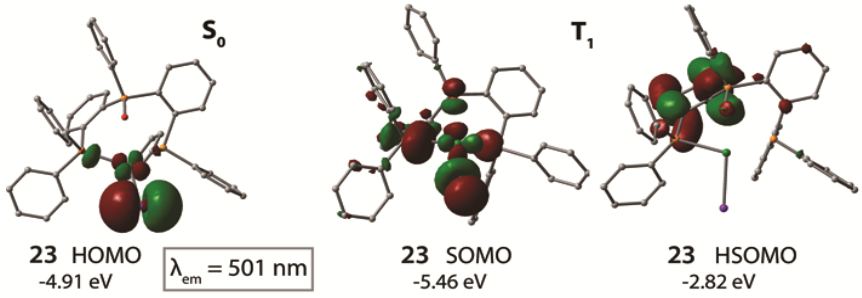

Figure 26. The appearance of the highest occupied orbitals in the S_0 ground state and the lowest excited triplet state of complex **23**. The emission wavelength was estimated from the total energy difference of the states.

*Dinuclear complexes [M₂(**P(PO)P**)₂]²⁺*. Coupling the **P(PO)P** ligand with two equivalents of the corresponding metal salts (Scheme 8) produced the dinuclear compounds $[M_2(\mathbf{P(PO)P})_2]^{2+}$ (M = Cu (**24**), Ag (**25**)). Modification of this procedure

that implies the reaction of AuCl(tht) (tht = tetrahydrothiophene) with **P(PO)P** phosphine and subtraction of chlorides with $AgPF_6$ was carried out to prepare the complex $[Au_2(\mathbf{P(PO)P})_2](PF_6)_2$ (**26**). The heterometallic congener $[AuCu(\mathbf{P(PO)P})_2](PF_6)_2$ (**27**) was isolated from the mixture of the equimolar amounts of homonuclear compounds **24** and **26**.

In **24**, a distorted tetrahedral coordination geometry was found for the copper centers (Fig. 27). The metal ions bind both **P(PO)P** ligands in a POP tridentate mode to form a chair-like $P(PO)PCu_2P(PO)P$ framework, where the Cu–O distances are nearly equal (2.121 and 2.198 Å).

In contrast to **24**, visibly unsymmetrical contacts between the Ag and oxygen atoms can be seen in **25**. Two terminal phosphorus donors and the O-atom are connected to each metal center. Additionally, moderately weak Ag–η^2(C=C) bondings[71] appear in crystal structure **25** with Ag(1)–C(1) and Ag(1)–C(2) distances of 2.954 and 2.822 Å, respectively, which reflect a tendency of silver(I) ions to adopt a four-coordinate arrangement of the ligand sphere.

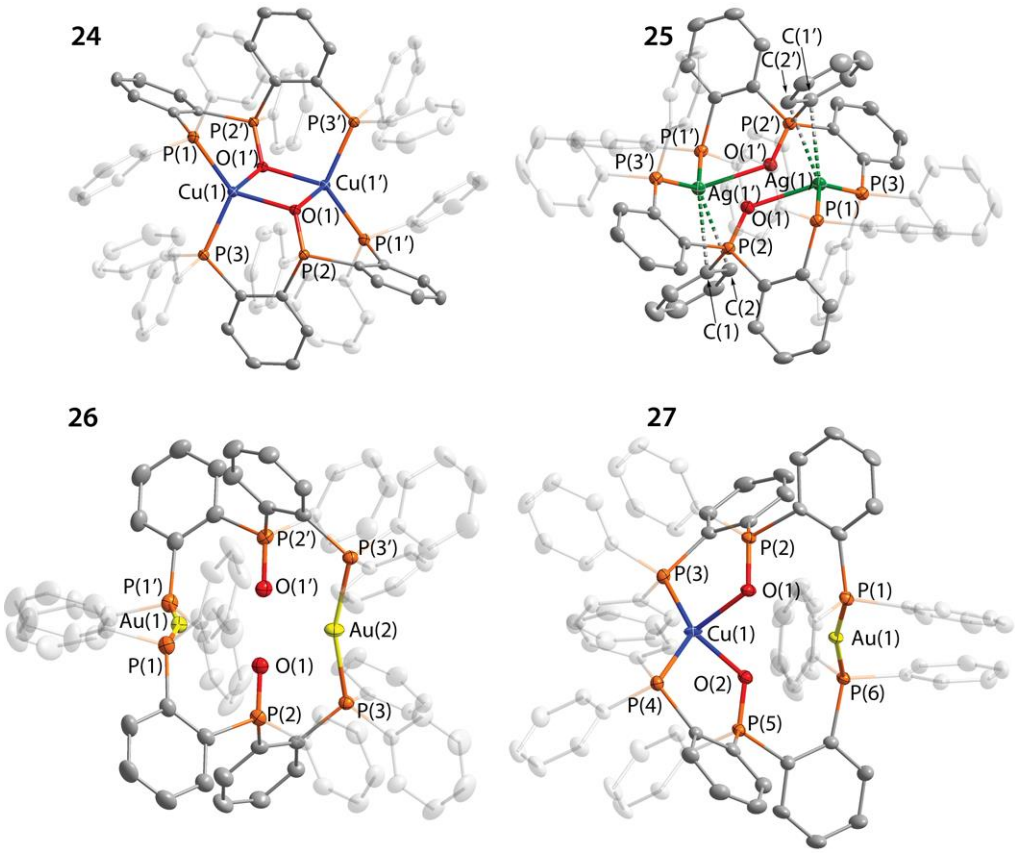

Figure 27. Molecular views of complexes **24**–**27**. Thermal ellipsoids are shown at the 50% probability level.

In digold complex **26**, the metal ions were found in a two-coordinate environment, typical for Au(I) complexes.[15] The P–Au–P angles deviate from linearity (164.3 and 159.8°) possibly due to weak Au···O interactions in the crystalline state (Au–O distances are 2.986 and 2.745 Å) that reflects a higher affinity of Au(I) ions to soft donors and a lower coordination number of gold(I) with respect to silver and copper.[23] In heterobimetallic complex **27**, two types of ligand arrangements ("P_2O_2" and "P_2") saturate the corresponding numbers of the coordination sites of Cu(I) and Au(I) ions, respectively.

The ESI-MS and NMR spectroscopic data in solution confirm the compositions and structures of complexes **24**–**26**. However, in fluid medium **27** there is a mixture of three compounds **24**, **26** and **27** which are in dynamic equilibrium, as indicated by its $^{31}P\{^1H\}$ NMR spectrum (Fig. 28) and by comparing against the spectroscopic patterns found for the individual species **24** and **26**. The unique set of three signals, which correspond to phosphine oxide (δ 45.3 dd, J_{PP} 11.2, 10.7 Hz) and PPh_2 groups bound to gold (δ 42.8 s) and copper (δ –12.3 br) ions, is completely compatible with the structure of **27**.

According to the computational analysis, the nature of the metal–ligand interactions reveals a clear trend for the strength of the M···O bonds, Cu > Ag > Au. On the other hand, an opposite trend is shown in the M–P bonds, Au > Ag > Cu.

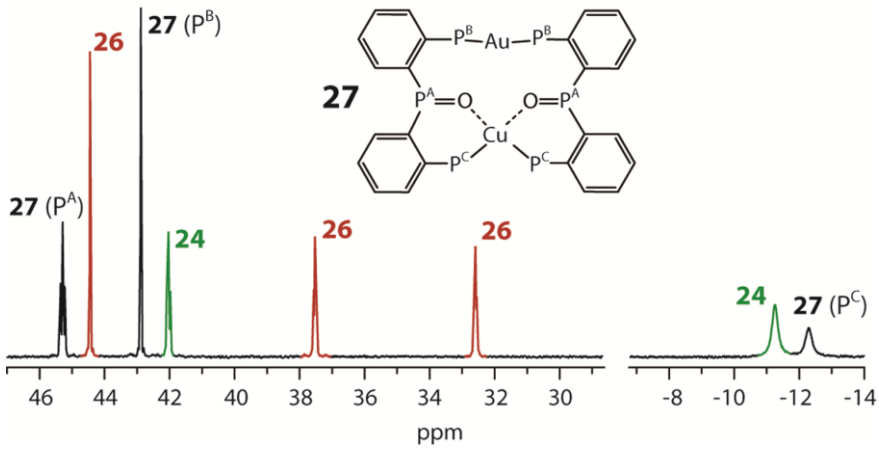

Figure 28. 162 MHz $^{31}P\{^1H\}$ NMR spectrum of the equilibrated mixture of compounds found in solution of **27** (DMSO-d_6, 298 K). The relative molar ratio of **24**:**26**:**27** is *ca*. 1:1:1.

Similarly to **20**–**23**, the photophysical properties of **24**–**27** were studied for the neat microcrystalline powders due to their extremely faint emission in solution. The dinuclear copper (**24**) and silver (**25**) complexes exhibit weak room temperature luminescence with broad peaks maximized at 604 (Φ_{em} 0.5%) and 500 nm (Φ_{em} 5.9%), respectively (Table 6). Lowering the temperature to 77 K does not affect the energy of the emission for **24** and leads to some blue shift for **25**. Considerably higher quantum yields (Φ_{em} 28.9 and 25.8%) were obtained for the Au-containing complexes with

emission bands centered at 548 (**26**) and 538 (**27**) nm. The lifetimes for **24**–**27** lie in the microsecond domain at 298 K and display a dramatic increase upon cooling to 77 K, reaching the value of 2354.3 μs (**25**, 216-fold increase). This behaviour correlates with that of some $[Ag(diphosphine)_2]^+$ compounds.[72]

Table 6. Solid state photophysical properties of **24**–**27**.

	λ_{ex}, nm		λ_{em}, nm		τ_{obs}, μs[a]		Φ_{em}, %
	298 K	77 K	298 K	77 K	298 K	77 K	298 K
24	364	365	604	604	0.35	174.1	0.5
25	332	324	500	485	10.9	2354.3	5.9
26	330	325	548	564	6.7	82.3	28.9
27	360	363	538	546	5.5	777.5	25.8

3.3.2 Heterotrinuclear P(PO)P complexes

To widen the coordination chemistry of the **P(PO)P** ligand, it was probed for the preparation of heteronuclear d^{10} alkynyl clusters, which are often formed due to a π-bridging ability of the –C≡C– motif that stabilizes coinage metal aggregates.[36a,63a,73]

Reactions between coordinatively unsaturated species $[M(\mathbf{P(PO)P})]^+$, which were prepared *in situ* by treating $[Cu(NCMe)_4]^+$ or Ag^+ triflates with **P(PO)P** phosphine, and the anionic dialkynyl complexes $[Au(C_2R)_2]^-PPN^+$ (generated by the "acac method" of Vicente[74]) were carried out to produce the trimetallic clusters $[\{(\mathbf{P(PO)P})M\}_2Au(C_2R)_2]CF_3SO_3$ (**28**–**30**, Scheme 9). It should be noted that no similar compounds could be identified in the case of the non-oxidized **P(P)P** ligand.

Scheme 9. Synthesis of complexes **28**–**30** (CH_2Cl_2/ acetone, 3 h, 298 K).

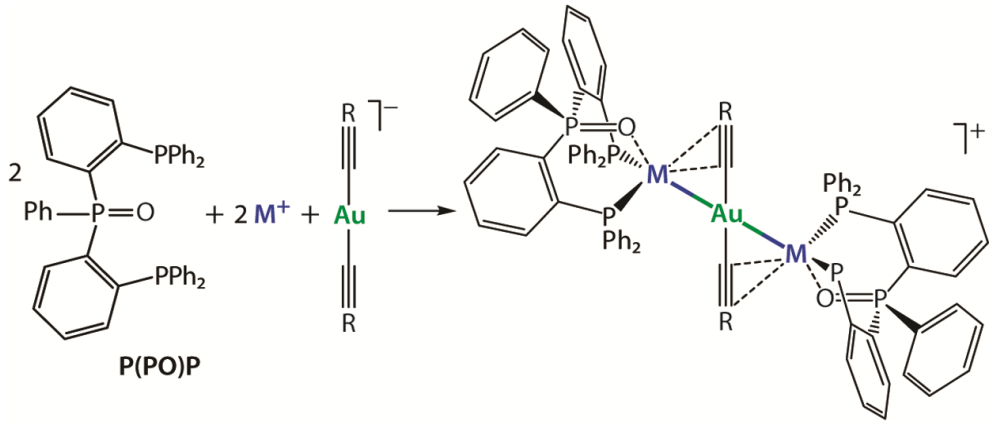

28 (M = Cu, R = C(OH)Ph$_2$), 67%
29 (M = Ag, R = C(OH)Ph$_2$), 56%
30 (M = Ag, R = Ph), 61%

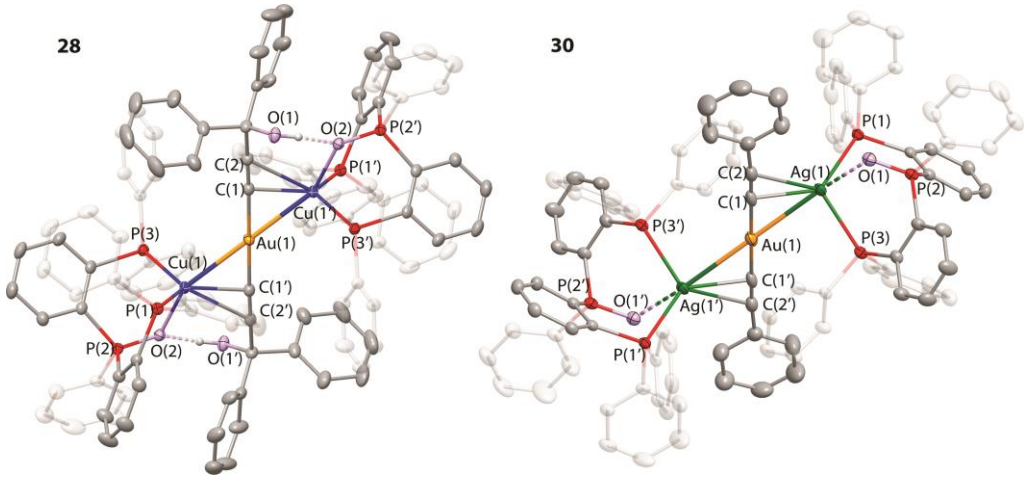

Figure 29. Molecular views of complexes **28** and **30**. Thermal ellipsoids are shown at the 50% probability level.

According to the XRD data, in **28**–**30** the gold (I) dialkynyl anion bears two cationic $[M(\boldsymbol{P^3O})]^+$ (M = Cu, Ag) units, which are assembled by means of the Au–M and π–C≡C–M (M = Cu, Ag) bonding (Fig. 29).

The ideal linear arrangements were found in the metal ion geometry and in the central dialkynyl gold unit $[Au(C_2R)_2]^-$ (M–Au–M and C(1)–Au–C(1´) angles are 180.0°). Similarly to **18**–**30**, rather weak M···O contacts are also observed in the structures of **28**–**30** (2.2384(17), 2.527(6), 2.624(3) Å, respectively). Interestingly, the effective –O–H···O=P hydrogen bonding was observed in **28** and **29**, which is indicated by short O(1)···O(2) distances (2.806 and 2.787 Å for **28** and **29**, respectively). These intramolecular interactions evidently result in additional stablization of these species.

The ESI-MS and NMR data indicate that **28**–**30** were preserved in solution. Their ^{31}P spectra display two signals with 1:2 intensities ratio, in the case of silver-containing compounds **28** and **29** typical $^{107/109}Ag$–^{31}P splittings were observed for the resonances of double intensity, corresponding to the equivalent metal-bound PPh_2 groups. The ^1H NMR spectra are also compatible with the solid state structures of **28**–**30**.

The optical properties of **28**–**30** were investigated in the solid state at 298 K and 77 K, but no appreciable luminescence was detected in solution. These complexes display weak to moderately intense phosphorescence (Φ_{em} up to 46%), which lie in the range from 481 to 532 nm under ambient conditions (Table 7).

Both the composition and structure of the metal core and the properties of the ligand sphere influence the photophysical behaviour of the titled compounds. In particular, the copper-containing cluster **28** displays a lower emission energy in comparison to the silver congeners **29** and **30,** while the electronic properties of the alkynyl –C≡CR groups used in these complexes show a less pronounced effect.

Table 7. Solid state photophysical properties of **28**−**30**.

	298K				77K	
	λ_{ex}, nm	λ_{em}, nm	$\Phi(\%)$	τ_{av}, μs[a]	λ_{ex}, nm	λ_{em}, nm
28	372	532	30	2.5	365	523
29	330 sh, 365	485	~1	1.7	325	488
30	354, 400, 428	440, 481	46	5.2	332, 400, 415 432,	437, 458, 469, 482

[a] Average emission lifetime for all of the complexes, except **28,** for the two exponential decay determined by the equation $\tau_{av} = (A_1\tau_1^2 + A_2\tau_2^2)/(A_1\tau_1 + A_2\tau_2)$, A_i – weight of the *i*-exponent.

This red-shifted emission of **28** is in line with the previous heteronuclear Au-Cu/Ag complexes **12**, **13**, the compounds based on the same ligand **P(PO)P** (**18**−**25**)**,** and other related species reported in the literature.[31,75,76] The cluster-centered transitions mixed with some MLCT d→π*(alkyne) character are tentatively attributed to the excited states of complexes **28** and **29**, while a significant contribution of the ^{3}IL transitions in the emission of **30** is evidenced by the vibronic structure of the emission band, which is enhanced upon lowering the temperature from 77 K and shows progression with a Δν of *ca.* 1100 cm^{-1} corresponding to the vibrational modes of aromatic ligands.

4 CONCLUSIONS

In this study, the coordination chemistry of the polydentate phosphine ligands was investigated with respect to d^{10} coinage metal ions that resulted in the assembly of new families of small metal clusters.

In the first step, a systematic variation of ancillary alkynyl ligands was accomplished in the series of tetragold(I) clusters $[Au_4(C_2R)_2(\mathbf{PPP})_2]^{2+}$ supported by the tridentate ligand **PPP** (bis(diphenylphosphinomethyl)phenylphosphine). Two structural motifs, which feature rhomboidal and unprecedented T-shaped geometries, were observed for the metal frameworks in the solid state. These tetranuclear species demonstrate moderate to intense room temperature phosphorescence with a maximum quantum yield of 51%. A clear bathochromic shift of emission maxima was revealed upon the increase of the electron-donor ability of the alkynyl groups that results in a wide modulation of emission energy which covers the range from 443 nm (blue) to 615 nm (orange). Using cluster $[Au_4(C_2C_6H_4NMe_2)_2(\mathbf{PPP})_2]^{2+}$ as a dopant emitter, an electroluminescent device was fabricated for the first time for polynuclear gold(I) complexes. Concurrently, electrochemical studies of the congener ferrocenyl-functionalized species showed that the Au_4 core behaves as an effective mediator of charge mobility when decorated by rigid –C≡C–Fc fragments.

The successful synthesis of the homoleptic compounds based on tri- (**PPP**) and tetradentate (**PPPP**, tris(diphenylphosphinomethyl)phosphine) ligands allowed one to alter the composition of the metal framework. The title complexes exhibited linear trimetallic $[MM'_2(\mathbf{PPP})_2]^{3+}$ or planar star-shape tetrametallic structural patterns $[MM'_3(\mathbf{PPPP})_2]^{4+}$ in addition to the unique tetranuclear gold-copper structure $[Au_2Cu_2(NCMe)_2(\mathbf{PPPP})_2]^{4+}$. The photophysical behaviour of these compounds is dominated by the electronic transitions, located predominantly within the metal core and are thus assigned exclusively to the nature of the constituent metal ions. The variable emission energy (λ_{em} = 450–563 nm) and intensity (Φ_{em} = 6–64%) demonstrate a way to tune the luminescence parameters through changing the composition of the cluster framework, yet retaining the ligand environment.

Furthermore, the hybrid phosphine-phosphine oxide (**P**(**PO**)**P**) displayed an adjustable binding ability in the series of mono-, di- and trinuclear complexes, depending on the coordination preferences of the constituent metal ions. The effectiveness of M···O bonding revealed the trend Cu > Ag > Au. The P-oxide group caused a substantial blue shift of the emission maxima in silver [AgHal**P**(**PO**)**P**] compounds, but largely quenched the emission of the Cu congeners. For the homoleptic species $[MM'(\mathbf{P}(\mathbf{PO})\mathbf{P})_2]^{2+}$, the highest quantum yield was achieved for the purely gold metal core, while combining the **P**(**PO**)**P** and the alkynyl ligands produced trinuclear clusters with diverse electronic transitions.

Altering the electronic properties of the bridging ligands, the composition and geometry of the metal core was shown to affect the structural patterns and optical behaviour of polynuclear d^{10} metal complexes, which constitute an intriguing class of inorganic and organometallic compounds with photophysical functionalities.

ACKNOWLEDGEMENTS

This work was carried out at the Department of Chemistry, University of Eastern Finland between 2013−2017. Financial support provided by the University of Eastern Finland and the Academy of Finland is gratefully acknowledged.

I am deeply grateful to my supervisor Professor Igor O. Koshevoy for introducing me to the interesting field of metal complexes, for sharing his knowledge, and for his invaluable guidance, motivational discussions and kind support throughout this work.

Special thanks are owed to the collaborative groups from the National Taiwan University (Taiwan, Prof. Pi-Tai Chou), St. Petersburg's State University (Russia, Prof. Sergey P. Tunik) and Aalto University (Finland, Prof. Antti J. Karttunen) for their effective cooperation. I sincerely thank Prof. Tapani Pakkanen, Docent Pipsa Hirva and Prof. Janne Jänis for their inspirational discussions and fruitful contributions towards my publications.

I also wish to thank the whole of my Inorganic Chemistry research group. In particular, I would like to thank Andrey Belyaev, MSc and Gomathy Chakkaradhari, MSc for their effective contributions towards my work. I am grateful to Ilya Kondrasenko, MSc and Vasily Sivchik, MSc for always being supportive of me. Andrey, Gomathy, Ilya and Vasily, whenever I needed help, you were always there for me. We had many valuable discussions on chemistry, I have learned many things from you all.

Thank you to all the colleagues and personnel at the Department of Chemistry for your pleasant, friendly working environment. Particularly, I would like to thank Prof. Tuula Pakkanen, Prof. Mika Suvanto, Prof. Juha Rouvinen, Sari Suvanto, Mari Heiskanen, Sirpa Jääskeläinen, Tarja Virrantalo, Taina Nivajärvi, Päivi Inkinen, Ritva Romppanen, Martti Lappalainen, Martti Varhimo, Janne Hirvi, Eija Faari-Kapanen, Tapani Venalainen and Urpo Ratinen for their continous encouragement and practical help in the department. I enjoyed all your positive attitudes and your senses of humor. Special thanks are also owed to Lin Lin Sun, Chian Ye Ling, Lena Ammosova, Anish Philip, Kristina Kisel, Kati Mielonen and Ville Nissinen for all the lively discussions and constant support.

I am grateful to my dear friends Trinh Thi Hoai Huong and Anastasia Naumkina, who have always been there for me, no matter what. Huong, whenever I heard you say "I am here, I am listening", it meant a great deal to me.

My warmest thanks go to my parents Tang and Thao, my sister Nguyet Minh, my dear cousin Dao, and my parents-in-law Tapsa and Mari. Your love, care and encouragement have given me strength to pursue my dreams. I am also deeply grateful to Leila Alvila and Kari Alvila for their love and support all along my journey. To me, you are more than teachers and friends, you are my family here. Last, but not least, my loving thanks go to my dearest husband Riku Saarenheimo and my sweet little girl Suvi Liisa Saarenheimo. You two are the best things in my life. Thank you all for supporting me through sad and good moments, life is lovely when I am with you.

Joensuu, September 2017 Dau Thuy Minh

5 REFERENCES

1. www.nobelprize.org.
2. (a) Crespo, O., Gold–Gold Interactions. In *Modern Supramolecular Gold Chemistry*, Laguna, A., Ed. Wiley-VCH: Weinheim, 2008; pp 65-131; (b) Fernandez, E. J.; Laguna, b.; Lopez-de-Luzuriaga, J. M., *Dalton Trans.* **2007**, 1969-1981; (c) Silvestru, C., Gold-Heterometal Interactions and Bonds. In *Modern Supramolecular Gold Chemistry*, Laguna, A., Ed.; Wiley-VCH: Weinheim: 2008; pp 181-295.
3. Echavarren, A. M.; Jiao, N.; Gevorgyan, V., *Chem. Soc. Rev.* **2016,** *45*, 4445.
4. (a) McKeage, M. J.; Maharaj, L.; Berners-Price, S. J. *Coord. Chem. Rev.* **2002,** *232*, 127-135; (b) Tiekink, E. R. T., **2002,** *42* 225-248; (c) Tiekink, E. R. T., *Inflammopharmacology* **2008,** *16*, 138-142; (d) Ott, I., *Coord. Chem. Rev.* **2009,** *253*, 1670-1681; (e) Che, C.-M.; Sun, R. W.-Y., *Chem. Commun.* **2011,** *47*, 9554-9560; (f) Gautier, A.; Cisnetti, F., *Metallomics* **2012,** *4*, 23-32.
5. (a) Assefa, Z.; McBurnett, B. G.; Staples, R. J.; Fackler, J. P. J.; Assmann, B.; Angermaier, K.; Schmidbaur, H., *Inorg. Chem.* **1995,** *34*, 75-83; (b) Assefa, Z.; McBurnett, B. G.; Staples, R. J.; Fackler, J. P. J., *Inorg. Chem.* **1995,** *34*, 4965-4972; (c) Lee, Y.-A.; Eisenberg, R., *J. Am. Chem. Soc.* **2003,** *125*, 7778-7779; (d) Ito, H.; Saito, T.; Oshima, N.; Kitamura, N.; Ishizaka, S.; Hinatsu, Y.; Wakeshima, M.; Kato, M.; Tsuge, K.; Sawamura, M., *J. Am. Chem. Soc.* **2008,** *130*, 10044-10045; (e) Strasser, C. E.; Catalano, V. J., *J. Am. Chem. Soc.* **2010,** *132*, 10009-10011; (f) Deák, A.; Jobbágy, C.; Marsi, G.; Molnár, M.; Szakács, Z.; Baranyai, P., *Chem. Eur. J.* **2015,** *21*, 11495 - 11508.
6. (a) Fernández, E. J.; López-de-Luzuriaga, J. M..; Monge, M.; Montiel, M.; Olmos, M. E.; Pérez, J., *Inorg. Chem.* **2004,** *43*, 3573-3581; (b) Laguna, A.; Lasanta, T.; Lopez-de-Luzuriaga, J. M.; Monge, M.; Naumov, P.; Olmos, M. E., *J. Am. Chem. Soc.* **2010,** *132*, 456-457.
7. (a) Cariati, E.; Bu, X.; Ford, P. C., *Chem. Mater.* **2000,** *12*, 3385-3391; (b) Koshevoy, I. O.; Chang, Y.-C.; Karttunen, A. J.; Haukka, M.; Pakkanen, T.; Chou, P.-T., *J. Am. Chem. Soc.* **2012,** *134*, 6564−6567.
8. (a) Rehr, J. J.; Zaremba, E.; Kohn, W., *Phys. Rev. B.* **1975,** *12*, 2062-2066; (b) Sadler, P. J., *Struct. Bonding* **1976,** *29*, 171-214.
9. Yam, V. W.-W.; Cheng, E. C.-C., *Chem. Soc. Rev.* **2008,** *37*, 1806-1813.
10. Scherbaum, F.; Grohmann, A.; Huber, B.; Kruger, C.; Schmidbaur, H., *Angew. Chem. Int. Ed. Engl.* **1988,** *27* (11), 1544-1546.
11. Pyykkö, P., *Chem. Rev.* **1997,** *97*, 597-636.
12. Pyykkö, P.; Zhao, Y., *Angew. Chem. Int. Ed. Engl.* **1991,** *30*, 604−605.
13. Pyykko, P., *Angew. Chem. Int. Ed.* **2004,** *43*, 4412-4456.
14. London, F., *Trans. Faraday Soc.* **1937,** *33*, 8-26.
15. Gimeno, M. C., The Chemistry of Gold. In *Modern Supramolecular Gold Chemistry*, Laguna, A., Ed.; Wiley-VCH: Weinhem, 2008; pp 1-64.
16. Pyykkö, P., *Chem. Rev.* **1988,** *88*, 563-594.

17. (a) Mayers, D. F., *Proc. R. Soc. (London)* **1957**, *Ser. A241*, 93; (b) Boyd, R. G.; Larson, A. C.; Waber, J. T., *Phys. Rev.* **1963,** *129*, 1629.

18. Pyykkö, P.; Li, J.; Runeberg, N., *Chem. Phys. Lett.* **1994,** *218* (1, 2), 133-138.

19. (a) Pyykkö, P.; Zhao, Y.-F., *Angew. Chem. Int. Ed. Engl.* **1991**, 30, 5, 604-605; (b) Li, J.; Pyykkö, P., *Chem. Phys. Lett.* **1992,** *197*, 586; (c) Li, J.; Pyykkö, P., *Inorg. Chem.* **1993,** *32*, 2630-2634; (d) Fernández, E. J.; Lopez-de-Luzuriaga, J. M.; Monge, M.; Rodríguez, M. A.; Crespo, O.; Gimeno, M. C.; Laguna, A.; Jones, P. G., *Inorg. Chem.* **1998,** *37*, 6002-6006.

20. Fernandez, E. J.; Lopez-de-Luzuriaga, J. M.; Monge, M.; Rodriguez, M. A.; Crespo, O.; Gimeno, M. C.; Laguna, A.; Jones, P. G., *Chem. Eur. J.* **2000,** *6*, 636-644.

21. (a) Silvestru, C., Gold-Heterometal Interactions and Bonds. In *Modern Supramolecular Gold Chemistry*, Laguna, A., Ed.; Wiley-VCH: Weinheim: 2008; p 260-272; (b) Che, C.-M.; Lai, S.-W., Luminescence and Photophysics of Gold Complexes. In *Gold Chemistry*, Mohr, F., Ed.; Wiley-VCH: Weinheim, 2009; pp 249-282.

22. (a) Schmidbaur, H.; Schier, A., *Chem. Soc. Rev.* **2012,** *41*, 370-412; (b) Schmidbaur, H.; Schier, A., *Angew. Chem. Int. Ed.* **2015,** *54*, 746 - 784.

23. Carvajal, M. A.; Novoa, J. J.; Alvarez, S., *J. Am. Chem. Soc.* **2004,** *126*, 1465-1477.

24. Fernandez, E. J.; Laguna, A.; Lopez-de-Luzuriaga, J. M.; Monge, M.; Montiel, M.; Olmos, M. E.; Rodrıguez-Castilloa, M., *Dalton Trans.* **2009**, 7509-7518.

25. Bardajı, M.; Calhorda, M. J.; Costa, P. J.; Jones, P. G.; Laguna, A.; Perez, M. R.; Villacampa, M. D., *Inorg. Chem.* **2006,** *45*, 1059-1068.

26. Blanco, M. C.; Camara, J.; Gimeno, M. C.; Jones, P. G.; Laguna, A.; Lopez-de-Luzuriaga, J. M.; Olmos, M. E.; Villacampa, M. D., *Organometallics* **2012,** *31*, 2597–2605.

27. Tong, G. S. M.; Kui, S. C. F.; Chao, H.-Y.; Zhu, N.; Che, C.-M., *Chem. Eur. J.* **2009,** *15*, 10777–10789.

28. Tanase, T.; Otaki, R.; Nishida, T.; Takenaka, H.; Takemura, Y.; Kure, B.; Nakajima, T.; Kitagawa, Y.; Tsubomura, T., *Chem. Eur. J.* **2014,** *20*, 1577 - 1596.

29. Ai, P.; Mauro, M.; Gourlaouen, C.; Carrara, S.; Cola, L. D.; Tobon, Y.; Giovanella, U.; Botta, C.; Danopoulos, A. A.; Braunstein, P., *Inorg. Chem.* **2016,** *55*, 8527−8542.

30. Catalano, V. J.; Kar, H. M.; Garnas, J., *Angew. Chem. Int. Ed.* **1999,** *38*, 1979−1982.

31. Krytchankou, I. S.; Krupenya, D. V.; Karttunen, A. J.; Tunik, S. P.; Pakkanen, T. A.; Chou, P.-T.; Koshevoy, I. O., *Dalton Trans.* **2014,** *43*, 3383-3394.

32. Jiang, Y.; Wang, Y.-T.; Ma, Z.-G.; Li, Z.-H.; Wei, Q.-H.; Chen, G.-N., *Organometallics* **2013,** *32*, 4919−4926.

33. Koshevoy, I. O.; Karttunen, A. J.; Kritchenkou, I. S.; Krupenya, D. V.; Selivanov, S. I.; Melnikov, A. S.; Tunik, S. P.; Haukka, M.; Pakkanen, T. A., *Inorg. Chem.* **2013,** *52*, 3663−3673.

34. Leznoff, D. B.; Xue, B.-Y.; Stevens, C. L.; Storr, A.; Thompson, R. C.; Patrick, B. O., *Polyhedron* **2001,** *20*, 1247-1254.

35. Yu, S.-Y.; Zhang, Z.-X.; Cheng, E. C.-C.; Li, Y.-Z.; Yam, V. W.-W.; Huang, H.-P.; Zhang, R., *J. Am. Chem. Soc.* **2005,** *127*, 17994-17995.

36. (a) Wang, Y.; Wan, X.-K.; Ren, L.; Su, H.; Li, G.; Malola, S.; Lin, S.; Tang, Z.; Häkkinen, H.; Teo, B. K.; Wang, Q.-M.; Zheng, N., *J. Am. Chem. Soc.* **2016,** *138*, 3278−3281; (b) Zeng, J.-L.; Guan, Z.-J.; Du, Y.; Nan, Z.-A.; Lin, Y.-M.; Wang, Q.-M., *J. Am. Chem. Soc.* **2016,** *138*, 7848−7851; (c) Lei, Z.; Wan, X.-K.; Yuan, S.-F.; Wanga, J.-Q.; Wang, Q.-M., *Dalton Trans.* **2017,** *46*, 3427-3434.

37. Wang, Y.; Su, H.; Xu, C.; Li, G.; Gell, L.; Lin, S.; Tang, Z.; Häkkinen, H.; Zheng, N., *J. Am. Chem. Soc.* **2015,** *137*, 4324−4327.

38. López-de-Luzuriaga, J. M., Luminescence of Supramolecular Gold-Containing Materials. In *Modern Supramolecular Gold Chemistry*, Laguna, A., Ed.; Wiley-VCH: Weinheim, 2008; pp 347-402.

39. Catalano, V. J.; López-de-Luzuriaga, J. M.; Monge, M.; Olmos, M. E.; Pascual, D., *Dalton Trans.* **2014,** *43*, 16486-16497.

40. Koshevoy, I. O.; Lin, C.-L.; Karttunen, A. J.; Jänis, J.; Haukka, M.; Tunik, S. P.; Chou, P.-T.; Pakkanen, T. A., *Chem. Eur. J.* **2011,** *17*, 11456 - 11466.

41. Xu, L.-J.; Wang, J.-Y.; Zhang, L.-Y.; Shi, L.-X.; Chen, Z.-N., *Organometallics* **2013,** *32*, 5402–5408.

42. (a) Ma, Y.; Che, C.-M.; Chao, H.-Y.; Zhou, X.; Chan, W.-H.; Shen, J., *Adv. Mater.* **1999,** *11* (10), 852-857; (b) Osawa, M.; Kawata, I.; Ishii, R.; Igawa, S.; Hashimoto, M.; Hoshino, M., *J. Mater. Chem. C* **2013,** *1*, 4375-4383; (c) Xu , L.-J.; Wang , J.-Y.; Zhu , X.-F.; Zeng , X.-C.; Chen, Z.-N., *Adv. Funct. Mater.* **2015,** *25*, 3033-3042; (d) Xu, L.-J.; Zhang, X.; Wang, J.-Y.; Chen, Z.-N., *J. Mater. Chem. C* **2016,** *4*, 1787-1794 ; (e) Zhang, F.; Guan, Y.; Chen, X.; Wang, S.; Liang, D.; Feng, Y.; Chen, S.; Li, S.; Li, Z.; Zhang, F.; Lu, C.; Cao, G.; Zhai, B., *Inorg. Chem.* **2017,** *56*, 3742−3753.

43. He, X.; Yam, V. W.-W., *Coord. Chem. Rev.* **2011,** *255*, 2111–2123.

44. (a) Zhao, Q.; Huang, C.; Li, F., *Chem. Soc. Rev.* **2011,** *40*, 2508-2524; (b) Koshevoy, I. O.; Lin, Y.-C.; Chen, Y.-C.; Karttunen, A. J.; Haukka, M.; Chou, P.-T.; Tunik, S. P.; Pakkanen, T. A., *Chem. Commun.* **2010,** *46*, 1440-1442; (c) Chelushkin, P. S.; Krupenya, D. V.; Tseng, Y.-J.; Kuo, T.-Y.; Chou, P.-T.; Koshevoy, I. O.; Burova, S. V.; Tunik, S. P., *Chem. Commun.* **2014,** *50*, 849--851.

45. (a) S. W. Botchway, M. C., J. W. Haycock, A. W. Parker,; D. L. Rochester, J. A. W. a. J. A. G. W., *Proc. Natl. Acad. Sci. U. S. A.* **2008,** *105*, 16071-16076; (b) Beeby, A.; Botchway, S. W.; Clarksona, I. M.; Faulknerc, S.; Parker, A. W.; Parker, D.; Williams, J. A. G., *J. Photochem. Photobiol. B, Biol.* **2000,** *57*, 83-89.

46. Seki, T.; Takamatsu, Y.; Ito, H., *J. Am. Chem. Soc.* **2016,** *138* (19), 6252-6260.

47. (a) Forward, J. M.; Bohmann, D.; Fackler, J. P. J.; Staples, R. J., *Inorg. Chem.* **1995,** *34*, 6330-6336; (b) Lagunas, M. C.; Fierro, C. M.; Pintado-Alba, A.; de la Riva, H.; Betanzos-Lara, S., *Gold Bull.* **2007,** *40*, 135-141; (c) Yam, V. W. W.; Cheng, E. C. C., *Top. Curr. Chem.* **2007,** *281*, 269-309; (d) Tiekink, E. R. T.; Kang, J.-G., *Coord. Chem. Rev.* **2009,** *253*, 1627–1648; (e) Lotito, K. J.; Peters, J. C., *Chem. Commun.* **2010,** *46*, 3690–3692; (f) Lima, J. C.; Rodriguez, L., *Chem. Soc. Rev.* **2011,** *40*, 5442–5456.

48. Appel, R.; Geisler, K.; Schöler, H.-F., *Chem. Ber.* **1979,** *112*, 648-653.

49. Campora, J.; Maya, C. M.; Matas, I.; Claasen, B.; Palma, P.; Alvarez, E., *Inorg. Chim. Acta*. **2006,** *359*, 3191−3196.

50. Raisanen, M. T.; Runeberg, N.; Klinga, M.; Nieger, M.; Bolte, M.; Pyykko, P.; Leskela, M.; Repo, T., *Inorg. Chem.* **2007,** *46*, 9954-9960.

51. (a) Coates, G. E.; Parkin, C., *J. Chem. Soc.* **1962**, 3220-3226; (b) Koshevoy, I. O.; Chang, Y.-C.; Karttunen, A. J.; Selivanov, S. I.; Jänis, J.; Haukka, M.; Pakkanen, T. A.; Tunik, S. P.; Chou, P.-T., *Inorg. Chem.* **2012,** *51*, 7392−7403.

52. Uson, R.; Laguna, A.; Laguna, M., *Inorg. Synth.* **1989,** *26*, 85-91.

53. (a) Yam, V. W.-W.; Cheung, K.-L.; Yip, S.-K.; Cheung, K.-K., *J. Organomet. Chem.* **2003,** *681* 196-209; (b) Koshevoy, I. O.; Chang, Y.-C.; Chen, Y.-A.; Karttunen, A. J.; Grachova, E. V.; Tunik, S. P.; Jänis, J.; Pakkanen, T. A.; Chou, P.-T., *Organometallics* **2014,** *33*, 2363-2371; (c) Yip, S.-K.; Lam, W. H.; Zhu, N.; Yam, V. W.-W., *Inorg. Chim. Acta* **2006,** *359*, 3639–3648; (d) Ho, S. Y.; Cheng, E. C.-C.; Tiekink, E. R. T.; Yam, V. W.-W., *Inorg. Chem.* **2006,** *45*, 8165-8174; (e) Han, S.; Yoon, Y. Y.; Jung, O.-S.; Lee, Y.-A., *Chem. Commun.* **2011,** *47*, 10689-10691.

54. Pyykkö, P., *Chem. Soc. Rev.* **2008,** *37*, 1967-1997.

55. Bardaji, M.; Laguna, A.; Orera, V. M.; Villacampa, M. D., *Inorg. Chem.* **1998,** *37*, 5125-5130.

56. (a) Koshevoy, I. O.; Lin, Y.-C.; Karttunen, A. J.; Chou, P.-T.; Vainiotalo, P.; Tunik, S. P.; Haukka, M.; Pakkanen, T. A., *Inorg. Chem.* **2009,** *48*, 2094-2102; (b) Zhang, L.-Y.; Xu, L.-J.; Zhang, X.; Wang, J.-Y.; Jia Li; Chen, Z.-N., *Inorg. Chem.* **2013,** *52*, 5167−5175.

57. (a) Ma, Y.; Che, C.-M.; Chao, H.-Y.; Zhou, X.; Chan, W.-H.; Shen, J., *Adv. Mater.* **1999,** *11*, 852-857; (b) Yam, V. W.-W.; Chan, C.-L.; Choi, S. W.-K.; Wong, K. M.-C.; Cheng, E. C.-C.; Yu, S.-C.; Ng, P.-K.; Chan, W.-K.; Cheung, K.-K., *Chem. Commun.* **2000**, 53-54; (c) Ma, Y.; Zhou, X.; Shen, J.; Chao, H.-Y.; Che, C.-M., *Appl. Phys. Lett.* **1999,** *74*, 1361-1363.

58. Xu, L.-J.; Zeng, X.-C.; Wang, J.-Y.; Zhang, L.-Y.; Chi, Y.; Chen, Z.-N., *ACS Appl. Mater. Interfaces* **2016,** *8*, 20251−20257.

59. (a) Xu, G.-L.; DeRosa, M. C.; Crutchley, R. J.; Ren, T., *J. Am. Chem. Soc.* **2004,** *126*, 3728-3729; (b) Ren, T., *Organometallics* **2005,** *24*, 4854-4870.

60. Albinati, A.; Biani, F. F. d.; Leoni, P.; Marchetti, L.; Pasquali, M.; Rizzato, S.; Zanello, P., *Angew. Chem. Int. Ed.* **2005,** *44*, 5701-5705.

61. Donoli, A.; Bisello, A.; Cardena, R.; Ceccon, A.; Bassetti, M.; D'Annibale, A.; Pasquini, C.; Raneri, A.; Santi, S., *Inorg. Chim. Act.* **2011,** *374*, 442-446.

62. Yam, V. W. W.; Au, V. K.-M.; Leung, S. Y.-L., *Chem. Rev.* **2015,** *115*, 7589−7728.

63. (a) Yam, V. W. W.; Lo, K. K.-W.; Wong, K. M.-C., *J. Organomet. Chem.* **1999,** *578*, 3-30; (b) Yam, V. W. W.; Wong, K. M. C., *Chem. Soc. Rev.* **1999,** *28*, 323–334; (c) Yam, V. W. W.; Wong, K. M. C., *Chem. Commun.* **2011,** *47*, 11579–11592.

64. (a) Che, C.-M.; Yip, H.-K.; Li, D.; Peng, S.-M.; Lee, G.-H.; Wang, Y.-M.; Liu, S.-T., *J. Chem. Soc., Chem. Commun.* **1991**, 1615-1617; (b) Koshevoy, I. O.; Shakirova, J. R.; Melnikov, A. S.; Haukka, M.; Tunik, S. P.; Pakkanen, T. A., *Dalton Trans.* **2011,** *40*, 7927-7933.

65. Slone, C. S.; Weinberg, D. A.; Mirkin, C. A., The Transition Metal Coordination Chemistry of Hemilabile Ligands, In *Progress in Inorganic Chemistry*, Karlin, K. D. Ed.; John Wiley & Sons: 1999; Vol. 48; pp 233-351.

66. Bader, A.; Lindner, E., *Coord. Chem. Rev.* **1991,** *108*, 27-110.

67. Angell, S. E.; Rogers, C. W.; Zhang, Y.; Wolf, M. O.; Jones Jr, W. E., *Coord. Chem. Rev.* **2006,** *250*, 1829-1841.

68. (a) Oliveri, C. G.; Ulmann, P. A.; Wiester, M. J.; Mirkin, C. A., *Acc. Chem. Res.* **2008,** *41*, 1618-1629; (b) Lifschitz, A. M.; Rosen, M. S.; McGuirk, C. M.; Mirkin, C. A., *J. Am. Chem. Soc.* **2015,** *137*, 7252-7261.

69. (a) Tsuboyama, A.; Kuge, K.; Furugori, M.; Okada, S.; Hoshino, M.; Ueno, K., *Inorg. Chem.* **2007,** *46*, 1992-2001; (b) Osawa, M.; Hoshino, M.; Hashimoto, M.; Kawata, I.; Igawa, S.; Yashima, M., *Dalton Trans.* **2015,** *44*, 8369–8378.

70. Derrah, E. J.; Martin, C.; Ladeira, S.; Miqueu, K.; Bouhadir, G.; Bourissou, D., *Dalton Trans.* **2012,** *41*, 14274.

71. Khlobystov, A. N.; Blake, A. J.; Champness, N. R.; Lemenovskii, D. A.; Majouga, A. G.; Zyk, N. V.; Schröder, M., *Coord. Chem. Rev.* **2001,** *222*, 155–192.

72. Matsumoto, K.; Shindo, T.; Mukasa, N.; Tsukuda, T.; Tsubomura, T., *Inorg. Chem.* **2010,** *49*, 805–814.

73. (a) Buschbeck, R.; Low, P. J.; Lang, H., *Coord. Chem. Rev.* **2011,** *255* 241-272; (b) Wang, Q.-M.; Lin, Y.-M.; Liu, K.-G., *Acc. Chem. Res.* **2015,** *48*, 1570−1579.

74. Vicente, J.; Chicote, M. T., *Coord. Chem. Rev.* **1999,** *193-195*, 1143–1161.

75. Frik, M.; Jimenez, J.; Gracia, I.; Falvello, L. R.; Habib, S. A.-.; Suriel, K.; Muth, T. R.; Contel, M., *Chem. Eur. J.* **2012,** *18*, 3659 - 3674.

76. Yip, S.-K.; Chan, C.-L.; Lam, W. H.; Cheung, K.-K.; Yam, V. W.-W., *Photochem. Photobiol. Sci.* **2007,** *6*, 365-371.

114/2012 LAURILA Elina: Non-covalent interactions in Rh, Ru, Os, and Ag complexes

115/2012 MAKSIMAINEN Mirko: Structural studies of *Trichoderma reesei*, *Aspergillus oryzae* and *Bacillus circulans* sp. *alkalophilus* beta-galactosidases – Novel insights into a structure-function relationship

116/2012 PÖLLÄNEN Maija: Morphological, thermal, mechanical, and tribological studies of polyethylene composites reinforced with micro– and nanofillers

117/2013 LAINE Anniina: Elementary reactions in metallocene/methylaluminoxane catalyzed polyolefin synthesis

118/2013 TIMONEN Juri: Synthesis, characterization and anti-inflammatory effects of substituted coumarin derivatives

119/2013 TAKKUNEN Laura: Three-dimensional roughness analysis for multiscale textured surfaces: Quantitative characterization and simulation of micro- and nanoscale structures

120/2014 STENBERG Henna: Studies of self-organizing layered coatings

121/2014 KEKÄLÄINEN Timo: Characterization of petroleum and bio-oil samples by ultrahigh-resolution Fourier transform ion cyclotron resonance mass spectrometry

122/2014 BAZHENOV Andrey: Towards deeper atomic-level understanding of the structure of magnesium dichloride and its performance as a support in the Ziegler-Natta catalytic system

123/2014 PIRINEN Sami: Studies on $MgCl_2$/ether supports in Ziegler–Natta catalysts for ethylene polymerization

124/2014 KORPELA Tarmo: Friction and wear of micro-structured polymer surfaces

125/2014 HUOVINEN Eero: Fabrication of hierarchically structured polymer surfaces

126/2014 EROLA Markus: Synthesis of colloidal gold and polymer particles and use of the particles in preparation of hierarchical structures with self-assembly

127/2015 KOSKINEN Laura: Structural and computational studies on the coordinative nature of halogen bonding

128/2015 TUIKKA Matti: Crystal engineering studies of barium bisphosphonates, iodine bridged ruthenium complexes, and copper chlorides

129/2015 JIANG Yu: Modification and applications of micro-structured polymer surfaces

130/2015 TABERMAN Helena: Structure and function of carbohydrate-modifying enzymes

131/2015 KUKLIN Mikhail S.: Towards optimization of metalocene olefin polymerization catalysts via structural modifications: a computational approach

132/2015 SALSTELA Janne: Influence of surface structuring on physical and mechanical properties of polymer-cellulose fiber composites and metal-polymer composite joints

133/2015 CHAUDRI Adil Maqsood: Tribological behavior of the polymers used in drug delivery devices

134/2015 HILLI Yulia: The structure-activity relationship of Pd-Ni three-way catalysts for H_2S suppression

135/2016 SUN Linlin: The effects of structural and environmental factors on the swelling behavior of Montmorillonite-Beidellite smectics: a molecular dynamics approach

136/2016 OFORI Albert: Inter- and intramolecular interactions in the stabilization and coordination of palladium and silver complexes: DFT and QTAIM studies

137/2016 LAVIKAINEN Lasse: The structure and surfaces of 2:1 phyllosilicate clay minerals

138/2016 MYLLER Antti T.: The effect of a coupling agent on the formation of area-selective monolayers of iron α-octabutoxy phthalocyanine on a nano-patterned titanium dioxide carrier

139/2016 KIRVESLAHTI Anna: Polymer wettability properties: their modification and influences upon water movement

140/2016 LAITAOJA Mikko: Structure-function studies of zinc proteins

141/2017 NISSINEN Ville: The roles of multidentate ether and amine electron donors in the crystal structure formation of magnesium chloride supports

142/2018 SAFDAR Muhammad: Manganese oxide based catalyzed micromotors: synthesis, characterization and applications